AUTONOMOUS UNMANNED AERIAL VEHICLE RENDEZVOUS FOR AUTOMATED AERIAL REFUELING

THESIS

Brian S. Burns, Major, USAF

AFIT/GAE/ENY/07- M05

DEPARTMENT OF THE AIR FORCE
AIR UNIVERSITY

AIR FORCE INSTITUTE OF TECHNOLOGY

Wright-Patterson Air Force Base, Ohio

AFIT/GAE/ENY/07- M05

AUTONOMOUS UNMANNED AERIAL VEHICLE RENDEZVOUS FOR AUTOMATED AERIAL REFUELING

THESIS

Presented to the Faculty

Department of Aeronautic and Astronautics

Graduate School of Engineering and Management

Air Force Institute of Technology

Air University

Air Education and Training Command

In Partial Fulfillment of the Requirements for the

Degree of Master of Science in Aeronautical Engineering

Brian S. Burns, BS, MBA

Major, USAF

March 2007

APPROVED FOR PUBLIC RELEASE; DISTRIBUTION UNLIMITED

AFIT/GAE/ENY/07- M05

AUTONOMOUS UNMANNED AERIAL VEHICLE RENDEZVOUS FOR AUTOMATED AERIAL REFUELING

Brian S. Burns, BS, MBA

Major, USAF

Approved:

Paul Blue
Major Paul A. Blue (Thesis Advisor) 16 Mar 07
Date

David R. Jacques
Dr. David R. Jacques (Committee Member) 16 MAR 07
Date

Dr. Richard G. Cobb (Committee Member) 16 MAR 07
Date

AFIT/GAE/ENY/07- M05

Abstract

As unmanned aerial vehicles (UAVs) increase in capability, the ability to refuel them in the air is becoming more critical. Aerial refueling will extend the range, shorten the response times, and extend the loiter time of UAVs. Executing aerial refueling autonomously will reduce the command and control, logistics, and training efforts associated with fielding UAV systems. Currently, the Air Force Research Laboratory is researching the various technologies required to conduct automated aerial refueling (AAR). One of the required technologies is the ability to autonomously rendezvous with the tanker. The goal of this research is to determine the control required to fly an optimum rendezvous using numerical optimization and to design a feedback controller that will approximate that optimal control.

Two problems were examined. The first problem is for the UAV receiver to rendezvous in minimum time, with a known tanker path. The second problem is for the receiver to rendezvous at a specified time with a known tanker path. For the first problem, the results of the rendezvous controller developed will be compared to the calculated optimal control.

Acknowledgments

I would like to express my sincere appreciation to my faculty advisor, Maj Paul Blue, for his guidance and support throughout the course of this thesis effort. His insight and experience were certainly appreciated. Additionally, without the support of the ANT Center staff and denizens of the ANT lab this effort would have been much less enjoyable. I would particularly like to thank Lt Zollars for his collaboration on our Dubins path code and Capt Rosario for his MATLAB expertise. Most of all, I would like to thank my family for their continuous support throughout this assignment.

Brian S. Burns

Table of Contents

Page

List of Figures

Page

Page

List of Tables

Page

(Page Left Blank)

AUTONOMOUS UNMANNED AERIAL VEHICLE RENDEZVOUS FOR AUTOMATED AERIAL REFUELING

1. Introduction

1.1. Motivation

Despite an initial resistance to unmanned aerial vehicles (UAVs), the U.S. Department of Defense (DOD) has realized that the use of UAVs provides a necessary capability. Since the somewhat recent introduction of large unmanned aerial vehicles into the DOD inventory, their capabilities have been rapidly expanding. One area of expansion has been an increased level of autonomy. For example, the Global Hawk system can taxi, fly, and land autonomously; the operator creates a preprogrammed route of flight and the Global Hawk system will fly the entire course without intervention. An important aspect of autonomy for UAVs would be the ability to perform aerial refueling; however, at this time, UAVs are not capable of aerial refueling.

The DOD has determined that the ability to autonomously refuel unmanned combat vehicles in the air is a requirement. Subsequently the Air Force Research Laboratory has initiated research into technologies that will enable automated aerial refueling (AAR). More generally, as UAVs increase in capability, the ability to refuel them in the air will become more critical. Aerial refueling will extend the range, shorten the response times, and extend loiter time of UAVs. Additionally, it will lessen the logistical effort necessary to deploy them by allowing fewer assets to perform the same mission and reducing the need for forward basing. Aerial refueling will greatly increase the capability of UAVs while allowing them to retain their small size and light weight.

1.2. Problem Definition

The goal of this research is to create a controller that navigates a receiver to effect a rendezvous with a tanker in a near optimal fashion. Since optimality depends on the specific cost function there are any number of optimal solutions. Therefore it is necessary to identify the cost function. There are many possible candidates to choose from. Energy expended could be minimized, fuel burned could be minimized, even more sophisticated cost functions which include life cycle cost based on aerodynamic loads or fatigue to rotating engine parts based on rpm changes, and finally, operational factors could contribute to the cost function. Many of these cost functions require knowledge of the specific receiver, therefore, while more sophisticated platform specific cost functions could be considered, this effort focused on two fairly generic problems. The first problem is an attempt to approximate the minimum fuel rendezvous, by minimizing the time for the receiver to rendezvous with the tanker. The assumption is that for many conditions, most notably tail chase scenarios, it may be more beneficial to increase the fuel flow rate for a short period of time in order to spend much less time in reaching the tanker. Clearly, before being implemented on a specific system, any algorithm would have to take the specific parameters of that system into account. However, the minimum time problem provides a first order approximation of the minimum fuel problem. The second problem addresses an operational issue. During large scale refueling operations, each receiver may have a specific time slot at which it is assigned to refuel. Since there is no benefit to arrive early and in fact arriving early may unnecessarily overcrowd the airspace surrounding the tanker, it is likely that it is optimal to arrive exactly at the specified time. Therefore the second problem is for the receiver to rendezvous at a specified time. One thing that must be taken into account no

matter what cost function is chosen, the terminal conditions at rendezvous must be met. Therefore, in both problems, the receiver must navigate from its initial position to a rendezvous point behind the tanker, while matching the tanker's heading, and airspeed at the rendezvous point.

1.3. Significance of Research

This research will provide the United States Air Force with an option to pursue in the quest for an air refuelable UAV. Current methodologies do not address varying airspeed and do not adequately address required time of arrival rendezvous. The approach taken here will be to further restrict the turn radius of the receiver to aid in achieving the required time of arrival (RTA). The intended effects will be to create the required delay, while also minimizing control energy. An additional benefit of this approach will be to keep the receiver in close proximity and in a favorable geometry so that if the required time of arrival changes or if the there were a delaying disturbance, the receiver would be poised to meet the new intercept condition.

1.4. Proposed solution

The proposed solution is to use a geometric approach to predict the location of the rendezvous point and to use a feedback controller to create acceleration and turn rate commands to guide the receiver to this intercept point with the required rendezvous conditions, heading and airspeed. This approach will be used for both problems. Additionally, for the second problem, the controller will artificially restrict the turn rate in order to assist in meeting the required time of arrival.

1.5. Related research

1.5.1. Optimal Path Planning

Since minimizing the time to travel to a point is related to minimizing the distance traveled to the point, literature on this topic was reviewed. Dr. L. E. Dubins proved that shortest path between point and orientation to point and orientation with constrained turn rate at constant velocity consists of no more than three segments and that the segments will either be straight lines or minimum radius turns. Additional research has been derived from the work of Dubins, for example, Xuan-Nam Bui, Jean-Daniel Boissonnat, Philippe Soueres, and Jean-Paul Laumond have presented a method to compute partitions for the horizontal plane [Bui 1994]. This method may be useful in reducing computation time required to calculate Dubins paths. Particularly applicable to this research is the work of Timothy McGee, Stephen Spry, and J Karl Hedrick, who propose a method for the generation of optimal paths in wind [McGee 2007].

1.5.2. Automated aerial refueling

Very little has been published regarding automated aerial refueling. Yoshimasa Ochi and Takeshi Kominami have proposed design methods for flight control systems based on proportional navigation guidance and line of sight angle control. Both these methods are for use once the receiver is in position behind the tanker [Ochi 2005]. Work has also been done by the USAF's Air Force Research Laboratory. Austin Smith has studied the use of proportional navigation guidance with adaptive terminal guidance in order to affect rendezvous. His methodology uses a tanker estimator to predict the rendezvous location, then uses proportional navigation to create a heading rate command to align the UAV's

heading with the tanker prior to rendezvous [Smith 2006]. Additionally, Steve Ross of the Air Force Institute of Technology has demonstrated a controller that was able to hold a Calspan owned Learjet LJ-25 with a variable stability system in the precontact and wing observation positions and to move between these positions [Ross 2006].

1.6. Thesis Overview

Chapter 2 will describe the mathematics, procedures, and tools used and provide the problem formulation. Additionally it will provide background on aerial refueling and list assumptions. Chapter 3 will detail the methods used and describe the models that were built. Chapter 4 will present the rendezvous controller developed for AAR and analyze the results of the simulations used to demonstrate its performance. Chapter 5 will present conclusions and make recommendations for future research.

2. Background and Problem Formulation

2.1. Overview

In this chapter, the various aspects of the research and its terminology will be introduced. These include aerial refueling, non-dimensionalization, the receiver's equations of motion, dynamic optimization, geometric path planning, dynamic inversions, numeric and simulation tools rendezvous controller, and assumptions. After introducing all of the components required, the two rendezvous problems being investigated are formulated.

2.2. Aerial Refueling

The ability for any air vehicle to perform its mission is limited by its supply of fuel. Additional fuel increases range, payload, and loiter time of aircraft [USAF 2003]. The act of transferring fuel from one aircraft to another is referred to as aerial refueling (AR) [DOD 2006]. By increasing range or endurance, AR can make missions possible that otherwise would not be. By allowing an increase in payload of the receiver, AR allows more missions to take place with a fixed number of aircraft [USAF 2003].

Prior to transfer of fuel, the aircraft must first rendezvous. There are two general ways aircraft involved in AR rendezvous, anchor or track [DOD 2006]. The anchor AR method is typically used when the amount of airspace available is restricted. When employing anchor AR, the tanker flies a small racetrack, while the receiver flies inbound on one of the legs of the racetrack, the tanker then rolls out in front of the receiver. See Figure 2-1. After rendezvous, the tanker flies a larger racetrack. For highly maneuverable receivers, such as fighter aircraft, the tanker aircraft will fly a highly predictable pattern and the receiver aircraft will effect the rendezvous. This type of rendezvous is referred to as a

fighter turn-on. See Figure 2-2. During large scale refueling operations, the tanker may continually fly the larger racetrack and receivers will perform the rendezvous. Aerial refueling tracks are a series of waypoints, usually located along the receiver's planned route of flight. With track AR, rendezvous is accomplished two ways. The first method is point parallel: in point parallel, the tanker orbits about a designated point, called the aerial refueling control point (ARCP), and waits for the receiver to arrive, then will rollout in front of the receiver. The second method is en route: in en route, the tanker and receiver arrive simultaneously at the ARCP. See Figure 2-3.

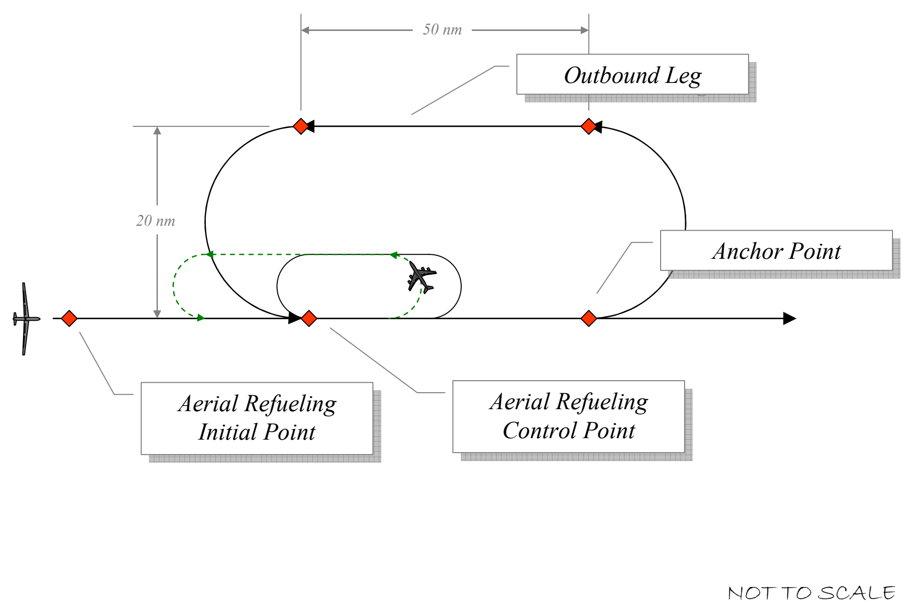

Figure 2-1 Aerial Refueling Anchor

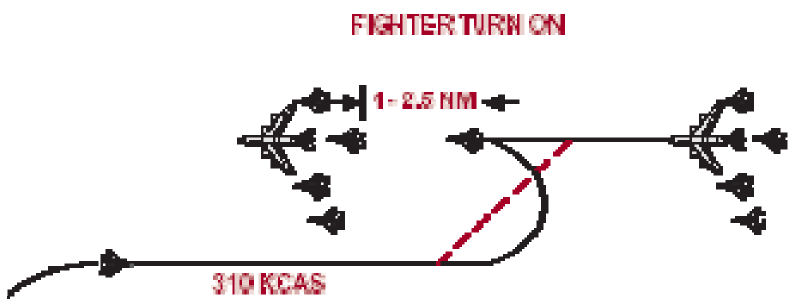

Figure 2-2 Fighter Turn-On [Neilsen 2005]

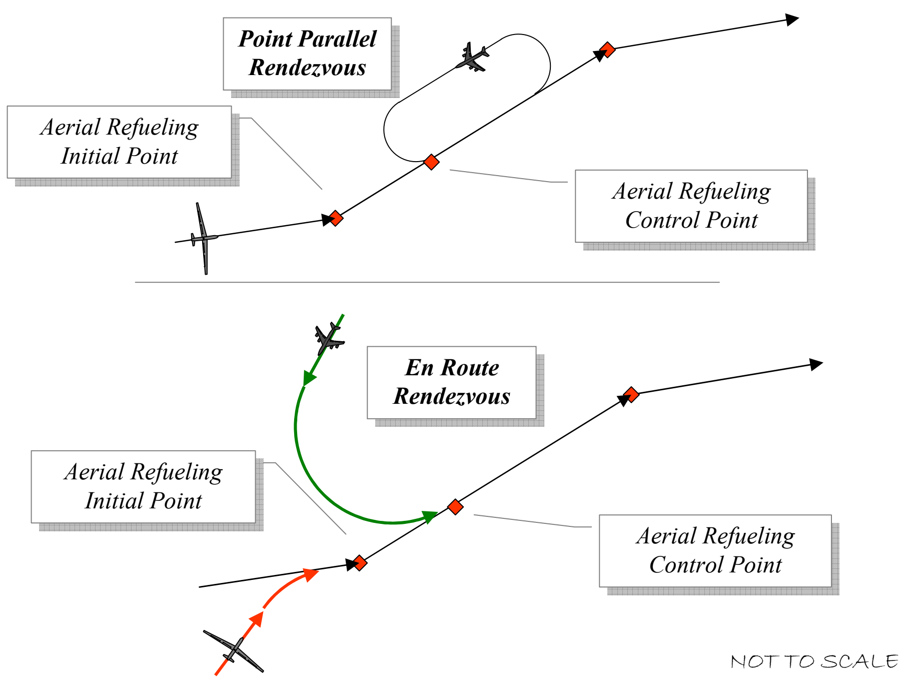

Figure 2-3 Aerial Refueling Track

It should also be noted that the receiver does not directly intercept the tanker, but a point directly behind the tanker (approximately 1-3 nm). Once the receiver has achieved this position it must wait until cleared by the tanker to approach the pre-contact position.

For the purpose of this work, the "mile-in-trail" position is the desired rendezvous point. Therefore, the term "tanker" and "rendezvous point" will be used interchangeably. See Figure 2-4.

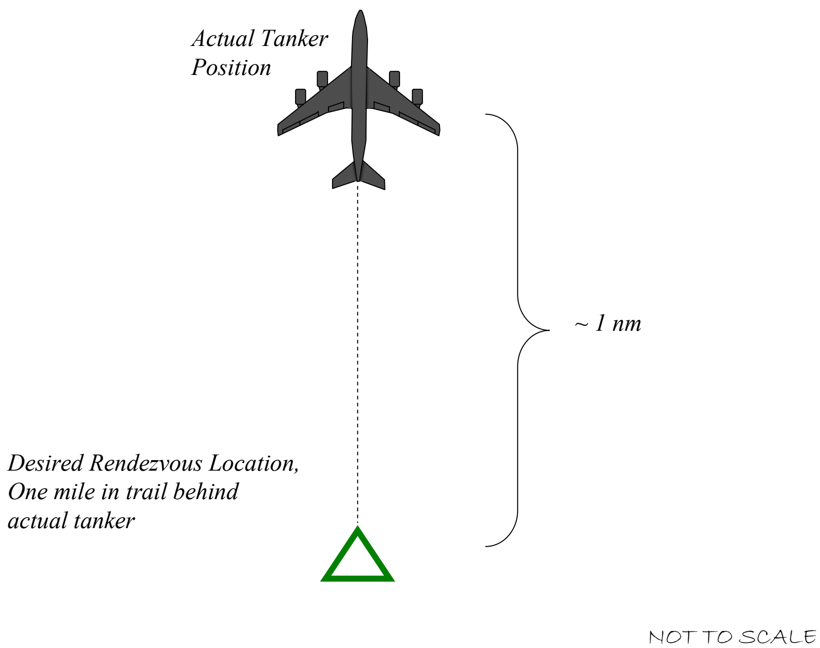

Figure 2-4 Rendezvous location

2.3. Non-dimensionalization

It is often useful to non-dimensionalize problems before attempting to solve them. Non-dimensionalization allows the solution to be applied to an entire class of problems, rather than just the originally posed problem. Non-dimensionalization can have other benefits such as scaling the problem so that all the parameters are roughly the same magnitude. This can be extremely useful if the solution involves a numeric technique, particularly numeric differentiation.

The Buckingham Pi Theorem is frequently utilized in the non-dimensionalization of problems. When applying the Buckingham Pi Theorem, the number of fundamental quantities involved, k, is subtracted from the number of variables, n. The difference, p, is the number of dimensionless Pi groups required to describe the problem. See Equation (1).

$$p = n - k \tag{1}$$

An analysis was performed to non-dimensionalize the current problem. All the variables were identified and listed with their fundamental dimensions. See Table 2-1. By inspection of the units in Table 2-1, it can be seen that all the variables can be expressed using only two dimensions—time and distance. According to the Buckingham Pi Theorem, any parameters can be chosen for the characteristic dimensions, However, in this case, it is convenient to select the rendezvous velocity, V, and the minimum turn radius of the receiver, R, as the characteristic dimensions, since they are constant with respect to the problem geometry and with respect to any initial conditions. Using the Buckingham Pi Theorem, described above, the problem is now expressed in n minus k (where k is equal to two) dimensionless Pi groups. Table 2-1 provides a sample of the Pi groups used, however, it should be noted that any variable consisting of a combination of length and time dimensions will be expressed as a Pi group.

Table 2-1 Scaling

Parameters	SI Units	Dimensional Variables	Dimensionless Pi Groups
Turn Radius of the Receiver	m	R	-
Distance to Intercept	m	D	$\frac{D}{R}$
Rendezvous Velocity (Nominal or planned airspeed at time of rendezvous)	$\frac{\mathrm{m}}{\mathrm{s}}$	V	-
Velocity of Receiver (Current airspeed of the receiver)	$\frac{\mathrm{m}}{\mathrm{s}}$	V_R	$\frac{V_R}{V}$
Velocity of Tanker (Current airspeed of the tanker)	$\frac{\mathrm{m}}{\mathrm{s}}$	V_T	$\frac{V_T}{V}$
Time	s	t	$\frac{tV}{R}$
Acceleration	$\frac{\mathrm{m}}{\mathrm{s}^2}$	a	$\frac{aR}{V^2}$

2.4. System Equations of Motion

Before the controller can be built, a mathematical model of the system must be constructed. For simplicity, both the receiver and the tanker will be modeled with point mass equations of motion. See Equations (2) through.(9). The states of both models include the position vectors and the velocity vectors. The position vectors include the downrange component, N, and the crossrange component, E. The velocity vectors include the airspeed, V, and the heading, χ (measured positive clockwise from the N-axis). The controls are acceleration, a, and heading rate (i.e. turn rate), ω. The equations of motion of the receiver follow:

$$\dot{N}_R = V_R \cdot \cos \chi_R \tag{2}$$

$$\dot{E}_R = V_R \cdot \sin \chi_R \tag{3}$$

$$\dot{\chi}_R = \omega_R \tag{4}$$

$$\dot{V}_R = a_R \tag{5}$$

The equations of motion of the tanker are:

$$\dot{N}_T = V_T \cdot \cos \chi_T \tag{6}$$

$$\dot{E}_T = V_T \cdot \sin \chi_T \tag{7}$$

$$\dot{\chi}_T = \omega_T \tag{8}$$

$$\dot{V}_T = a_T \tag{9}$$

A point mass model of the receiver and tanker (rendezvous point) dynamics, including velocity and turn rate controllers for the receiver, were created in MATLAB's Simulink. The state vectors included the position vectors and the velocity vectors of each vehicle, Equations (10) and (12). The controls for both the receiver and the tanker were heading rate and velocity rate, Equations (11) and (13). The tanker is programmed to fly a

preprogrammed, known, flight plan. The receiver is controlled by a rendezvous controller designed to generate the desired controls to effect a near optimal rendezvous. Both the receiver and the tanker have dynamic constraints, which include upper bounds on the turn rates, upper and lower bounds on the acceleration, and upper and lower bounds on the airspeeds. These constraints can be found in Table 2-2.

The equations of motion follow:

$$x_R = \begin{Bmatrix} N_R \\ E_R \\ \chi_R \\ V_R \end{Bmatrix} \tag{10}$$

$$u_R = \begin{Bmatrix} \omega_R \\ a_R \end{Bmatrix} \tag{11}$$

$$x_T = \begin{Bmatrix} N_T \\ E_T \\ \chi_T \\ V_T \end{Bmatrix} \tag{12}$$

$$u_T = \begin{Bmatrix} \omega_T \\ a_T \end{Bmatrix} \tag{13}$$

Table 2-2 Design Parameters

Parameter	Min	Max
Receiver Heading Turn Rate	-.98	.98
Receiver Acceleration	-.05	.1
Receiver Airspeed	.7	1.2
Tanker Turn rate	-1	1
Tanker Acceleration	0	0
Tanker Airspeed	1	1

2.5. Dynamic Optimization

The goal of this research is to develop a near optimal controller. In order to claim that the controller is near optimal, the results of the controller must be compared to the optimal solution. The optimal solution will be produced using dynamic optimization.

Dynamic optimization is a technique used to solve for the inputs or controls that minimize a given cost function of a dynamic system. Dynamic optimization techniques formulated by Bryson and Ho [Bryson 1975] will be used to create a benchmark. That is, the solution from the rendezvous controller will be compared to the solution found by dynamic optimization, which is expected to be the optimal solution. Before the problem is solved using dynamic optimization, it will be discretized and the equations of motion will be enforced as constraints. Then, the problem will be solved using MATLAB's Optimization Toolbox, specifically, the *fmincon* function.

The fmincon function is an element of MATLAB's Optimization Toolbox that is designed to find the minimum of constrained, non-linear, scalar functions of several variables. It starts with a user supplied initial guess; then it uses sequential quadratic

programming and line searches to find a local minimum. For this research, the initial guess provided will be based on the control required to fly a Dubins path.

Because *fmincon* is a parameter optimization tool, the above continuous equations of motion, Equations (2)-(4), were discretized prior to implementation. The equations were discretized using Euler's first order method with a constant time step. Before the discretization, the differential equations of motion, Equations (2) through (4) were expressed in parametric form. See Equations (14) through (17).

$$N(t) = N(t_0) + \int_{t_0}^{t} \dot{N}(t)dt \tag{14}$$

$$E(t) = E(t_0) + \int_{t_0}^{t} \dot{E}(t)dt \tag{15}$$

$$\chi(t) = \chi(t_0) + \int_{t_0}^{t} \dot{\chi}(t)dt \tag{16}$$

$$V(t) = V(t_0) + \int_{t_0}^{t} \dot{V}(t)dt \tag{17}$$

The final discretized equations of motion were generated by substituting Equations (6) through (9) into the above parametric equations and propagating them over one time step, *Δt*. They are as follows:

$$N_R(i+1) = N_R(i) + \Delta t \cdot V_R \cdot \sin \chi_R(i) \tag{18}$$

$$E_R(i+1) = E_R(i) + \Delta t \cdot V_R \cdot \cos \chi_R(i) \tag{19}$$

$$\chi_R(i+1) = \chi_R(i) + \Delta t \cdot \omega_R(i) \tag{20}$$

$$V_R(i+1) = V_R(i) + \Delta t \cdot a_R(i) \tag{21}$$

2.6. Receiver Tanker Rendezvous

This section will present the mathematical formulation of the problems which are to be solved by the feedback controllers, namely, the minimum time rendezvous problem and the specified time rendezvous problem.

2.6.1. Minimum Time Problem

In this problem, the time to rendezvous, t_f, will be minimized. Using the notation of Bryson and Ho [Bryson 1975] and subscripted with *R* for receiver, *T* for tanker, and *f* for final, the problem is formulated as follows:

Minimize:

$$J = \phi \text{ where, } \phi = t_f \tag{22}$$

Subject to:

Receiver and Tanker Equations of Motion:

$$N(i+1) = N(i) + dt \cdot V \cdot \sin \chi(i) \tag{23}$$

$$E(i+1) = E(i) + dt \cdot V \cdot \cos \theta(i) \tag{24}$$

$$\chi(i+1) = \chi(i) + dt \cdot \omega(i) \tag{25}$$

$$V(i+1) = V(i) + dt \cdot a(i) \tag{26}$$

Terminal Constraints:

$$N_{R_f} = N_{T_f} \tag{27}$$

$$E_{R_f} = E_{T_f} \tag{28}$$

$$\chi_{R_f} = \chi_{T_f} \tag{29}$$

$$V_{R_f} = V_{T_f} \tag{30}$$

Control and State Constraints:

$$|\omega| \le \dot{\chi}_{\max} \tag{31}$$

$$\dot{V}_{\min} \le a \le \dot{V}_{\max} \tag{32}$$

$$V_{\min} \le V \le V_{\max} \tag{33}$$

2.6.2. *Specified Time Problem*

In this problem, the square of the difference between the required time of arrival (RTA) and the time to rendezvous will be minimized. The problem would be formulated as follows:

Minimize:

$$J = \phi \text{ where, } \phi = (RTA - t_f)^2 \tag{34}$$

Subject to:

Tanker and receiver equations of motion.

Terminal Constraints:

$$\chi_{R_f} = \chi_{T_f} \tag{35}$$

$$v_{R_f} = v_{T_f} \tag{36}$$

$$x_{R_f} = x_{T_f} \tag{37}$$

$$y_{R_f} = y_{T_f} \tag{38}$$

Control and State Constraints:

$$|\omega| \le \dot{\chi}_{\max} \tag{39}$$

$$\dot{V}_{\min} \le a \le \dot{V}_{\max} \tag{40}$$

$$V_{\min} \le V \le V_{\max} \tag{41}$$

2.7. Optimal Path Planning

As noted in Chapter One, the problem of minimizing the time to travel to a terminal point is related to the problem of minimizing the path length. For this problem, it is assumed that the minimum path length is also the path desired when minimizing travel time. Therefore the shortest feasible path will be used.

For vehicles with constrained turning radius it has been shown that the minimum path length from an initial point and orientation to a terminal point and orientation consists of straight line segments and arcs of minimum turn radius. Also, every possible shortest path can be represented as a sequence consisting of exactly three segments of lines and arcs, represented by primitives, R, L, and S, where R represents a right hand turn of minimum turn radius, L represents a left hand turn of minimum turn radius, and S represents a straight line segment. It can be seen that there are ten possible combinations of arcs and line segments (RSR, RSL, LSR, LSL, LRL, RLR, SLR, SRL, RLS, and LRS). However, L. E. Dubins proved that only these six sequences are possibly optimal: RSR, RSL, LSR, LSL, LRL, and RLR [Dubins 1957]. From Figure 2-5 and Figure 2-6, it can be seen that the last two cases, RLR and LRL can only be optimal when the initial point and the terminal point

are within four turn radii. By restricting the problem to only cases where the initial point and terminal point are separated by at least four radii, these two cases can be ignored. This leaves only the four cases with two arcs and one line segment. For this research, it will be assumed that the receiver initial point is separated from the intercept point by at least four radii or that the geometry does not require these types of paths due to alignment.

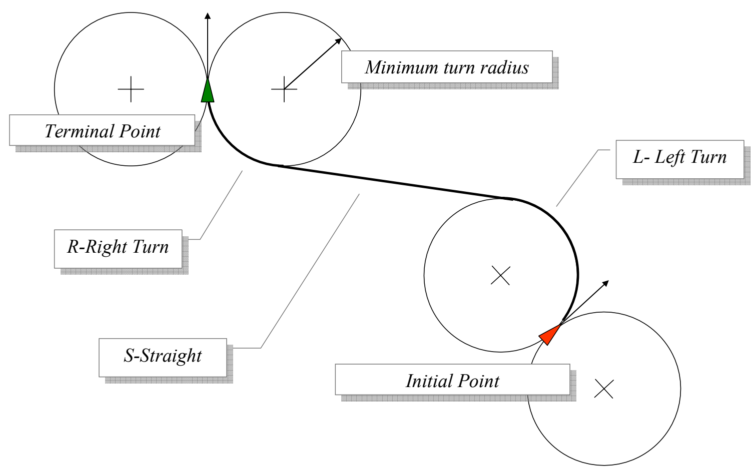

Figure 2-5 Sample LSR Dubins Path

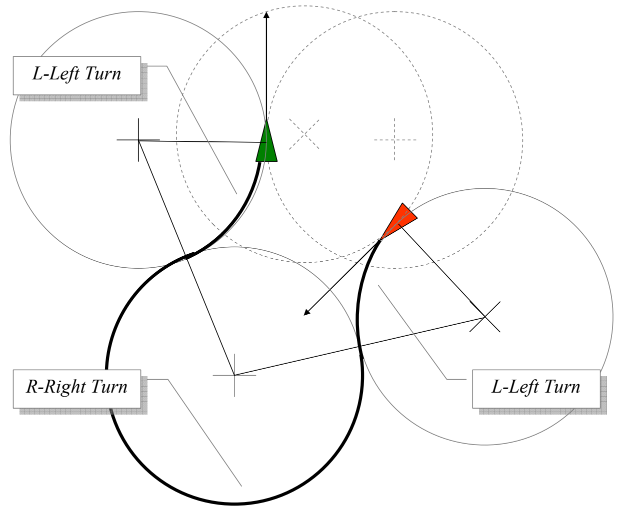

Figure 2-6 Sample LRL Dubins Path

2.8. Dynamic Inversion

Dynamic inversion is a non-linear control technique. It will be used in the rendezvous controller that will be designed. The purpose of the dynamic inversion controller is to compute a control command, u_{cmd}, such that the system response tracks the desired (commanded) response. When a properly designed dynamic inversion controller is used to command the system's control variables, it drives the system to respond, from dynamic inversion control input to system output, as an integrator [Wright Laboratories 1996]. Then, the input to the dynamic inversion controller is the desired rate of change of the system output to be controlled (control variable), which is referred to as the desired dynamics. A generic derivation showing how control is developed follows:

The equations of motion, Equations (2) through (4), can be expressed generically,

$$\dot{x} = f(x,u) \tag{42}$$

Likewise, a generic control variable, y, and its time derivate can be expressed,

$$y = h(x) \tag{43}$$

$$\dot{y} = \frac{\partial h}{\partial x}\dot{x} \tag{44}$$

By substitution,

$$\dot{y} = \frac{\partial h}{\partial x} f(x,u) \tag{45}$$

For clarity, a new function can be defined,

$$g \equiv \frac{\partial h}{\partial x} f(x,u) \tag{46}$$

Then, adding subscripts to explicitly show what the inputs and outputs of the dynamic inversion controller will be gives,

$$\dot{y}_{des} = g(x_{meas}, u_{cmd}) \tag{47}$$

Solving Equation (47) for u_{cmd}, gives the desired dynamic inversion controller, q, as a function of the measured states and the desired dynamics,

$$u_{cmd} = q(x_{meas}, \dot{y}_{des}) \tag{48}$$

2.9. Simulation Environment

The controller that will be designed will be built and simulated using MATLAB's Simulink package. Simulink is a MATLAB add-on that is designed for modeling and simulating linear or nonlinear dynamic systems [MATLAB 2005]. The models can be constructed using a graphical user interface to build block diagrams. The simulations can be run in continuous time by using one of several user defined numeric differential equation solvers.

2.10. Assumptions

The following assumptions have been made:

1. The problem is two dimensional; the receiver starts at and maintains the desired rendezvous altitude
2. The receiver will start sufficiently far from the desired rendezvous location such that only Circle-Line-Circle type paths are required.
3. A point mass model with heading and velocity control adequately represents the receiver's and tanker's motion for the purpose of path planning.
4. The receiver and the tanker experience the same winds.
5. The motion of the tanker is known.

2.11. Chapter Summary

In this chapter, background information was presented and the problem was formulated mathematically. The background information included aerial refueling, non-dimensionalization, dynamic optimization, optimal path planning, dynamic inversion, a description of the software tools to be used, and assumptions. The problem formulation included the non-dimensionalization scheme to be used and a mathematical expression of the problems to be solved.

3. Development of Optimal Trajectories and Control Laws

3.1. Overview

Two problems are being considered. The first is to design a controller that will provide turn rate and acceleration commands to a receiver in order to rendezvous with a tanker in the shortest period of time. The second is to design a similar controller that will provide commands to rendezvous with a tanker at a specified time. In both cases, the receiver must match its speed and heading with that of the tanker at the rendezvous point.

Both controllers will utilize a geometric approach, using the work of L. E. Dubins, as described above. The controller will calculate a Dubins path to the predicted intercept point. By inspection of Figure 3-1, it can be seen that in order for the UAV to fly the Dubins path, it must make a minimum radius turn in the direction of the heading of the straight segment. That is, it must turn toward the point where the line segment meets the second turn. This point will be called the predicted turn point. The receiver drives to the predicted turn point using a dynamic inversion controller that drives the receiver's projected miss distance to zero, where the projected miss distance is the perpendicular distance by which the receiver would miss the predicted turn point if it maintained its current heading. This control is applied until the UAV reaches the proximity of the predicted turn point, at which time it switches its aim point from the predicted turn point to the predicted intercept point. Once the simulations have been run, the overall times and control histories will be compared against the results of a numerical dynamic optimization routine.

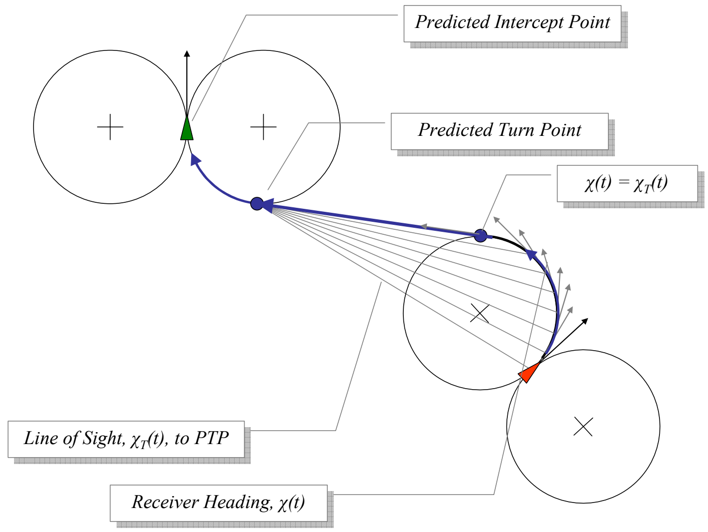

Figure 3-1 Receiver's Trajectory as Dubins Path

3.2. Geometric Waypoint Estimator

A geometric waypoint estimator is an integral part of the rendezvous controller. This waypoint estimator will generate waypoints for steering as well as estimate the path distance and time to rendezvous. The waypoint estimator relies on the work of L.E. Dubins and T. McGee, *et al*. As shown by L.E. Dubins [Dubins 1957], the optimal path in a two dimensional plane for a vehicle with a bounded turning radius from an initial position and heading to a terminal position and heading consists of straight line segments and minimum radius arcs. McGee *et al* have developed a method for optimal path planning in constant wind, which builds on Dubins' work [McGee 2007]. McGee's method makes the assumption that flying in a constant wind towards a target fixed to the ground is identical to flying towards a moving target without winds. The fixed target is replaced by a virtual target moving at the velocity of the wind, but in the opposite direction. For this problem, the

target is moving, so the virtual target is replaced by the real target which moves not at the velocity of the wind, but at its own airspeed. Wind is taken into account by fixing the coordinate system to the moving air mass as opposed to the ground. In McGee's method the wind is assumed to be constant, however, the assumption that the target moves with constant velocity is not necessary for this problem: either the future positions of the tanker as a function of time, $p_T(t)$, is known *a priori* through collaboration or it can be estimated, either by simply propagating the current state of the tanker or by more sophisticated means. In either case, the position of the tanker can be described as a function of time. That is, its trajectory is known or estimated and at each point on the trajectory, the time is known, Equation (49). For any time, it is possible to construct a Dubins path to this point and to compute the time required to traverse this path at a constant speed, Equation (51). The method requires the first occurrence of where the difference between these times is zero to be found; therefore, a new function, G, is defined as the difference of the times, Equation (52). The first zero of this function is the location of the minimum rendezvous time. [McGee 2007]

$$p_t = \begin{Bmatrix} x(t) \\ y(t) \end{Bmatrix} \tag{49}$$

$$T_t = T_t(x_t, y_t, v_t) \tag{50}$$

$$T_r = T_r(x_r, y_r, v_r) \tag{51}$$

$$G(x, y) \equiv T_r(x, y) - T_t(x, y) \tag{52}$$

McGee *et al* approach the method for finding the optimal path to rendezvous, but do not provide an implementable algorithm. For this research, an algorithm was developed using functions written in MATLAB, which are described in more detail in Appendix A and are available upon request by contacting the author. The algorithm iteratively finds the time to travel the Dubins path and the tanker's trajectory until a solution is found. The Dubins paths are generated from the receiver's initial position to a future tanker position. The paths are calculated by generating two pairs of circles, with radii equal to the minimum turn radius. One pair of circles is tangent to the initial velocity vector of the receiver and one pair is tangent to the future tanker position. See Figure 3-2. Lines tangent to each combination of initial and terminal circles are then constructed, resulting in four candidate paths. As long as the assumption that none of the circles overlap holds, the shortest of these paths is the Dubins path. See Figure 3-3. Overlapping circles would result in the possibility that the Dubins path consists of three minimum radius turns rather than two minimum radius turns and a straight segment. See Figure 3-4. As stated above, the goals of this algorithm are to produce steering waypoints and to find the path length and path time to intercept. Finding the Dubins path that achieves rendezvous satisfies these goals.

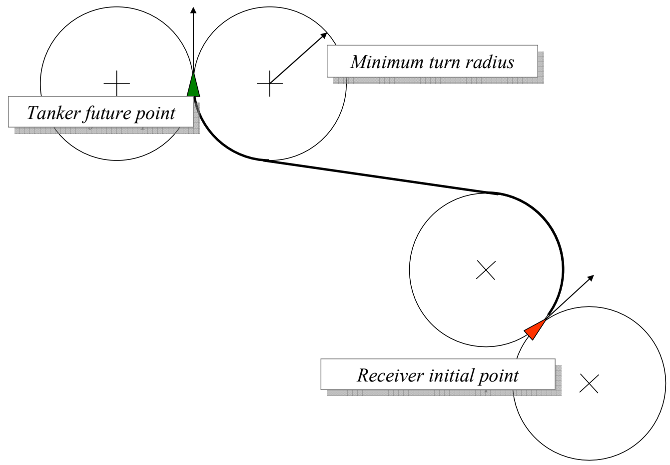

Figure 3-2 Construction of a Dubins Path

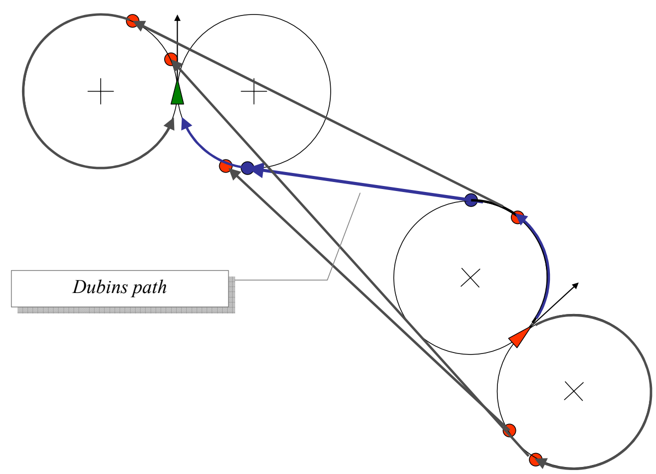

Figure 3-3 The Dubins Path is the Shortest of the four Candidate Paths

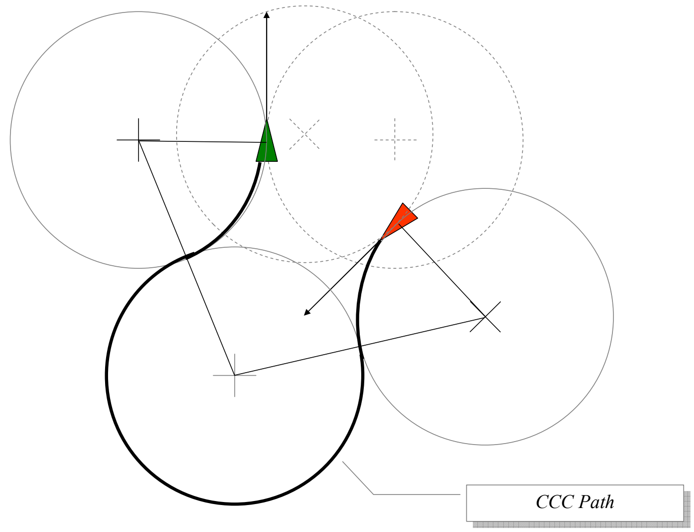

Figure 3-4 Dubins Path for Overlapping Circles

3.3. Development of Collaborative Autonomous Rendezvous Controller Model

3.3.1. Minimum Time Controller

The minimum time controller will generate heading rate and acceleration commands to achieve a rendezvous in minimum time. It accomplishes this through two control loops: a heading control loop and a velocity control loop.

<u>*Heading Controller*</u>

The heading controller uses a dynamic inversion controller to navigate to a series of two waypoints. The waypoints are generated using the Dubins path methodology, described above. First the dynamic inversion controller will be described then the mechanics of the entire heading control loop including the geometric waypoint estimator will be detailed.

The purpose of the dynamic inversion controller is to steer the receiver to waypoints by driving the miss distance, as shown in Figure 3-5, to zero. To create this controller, it was necessary to solve for the command, u, or more specifically, ω, as a function of the measured states and the desired response, such that the output of the controlled system is the integral of the input to the dynamic inversion (DI) controller. See Figure 3-5. The desired response in this case is to minimize the projected closest point of approach of the receiver's trajectory to the desired waypoint. The closest point of approach is the point on the receiver's current straight line path that passes closest to the target point. The closest point of approach is also called the miss distance and is represented by the variable m. See Figure 3-6. For this derivation, measured values will be denoted, "meas", commanded values, "cmd", and desired values, "des".

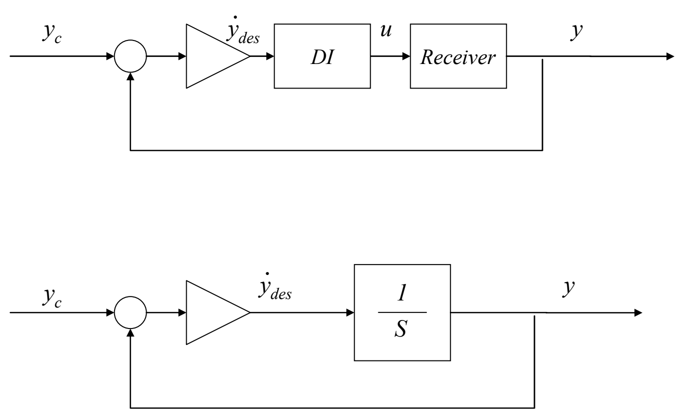

Figure 3-5 Dynamic Inversion Block Diagrams

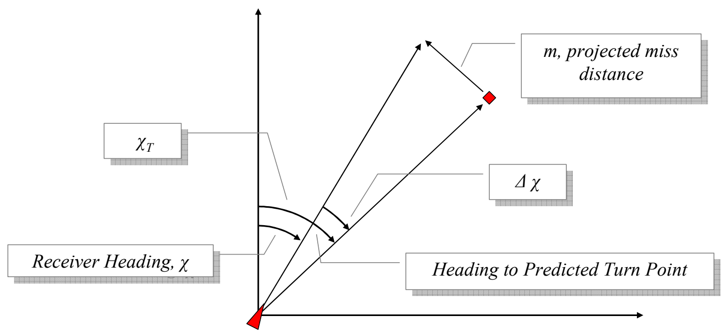

Figure 3-6 Dynamic Inversion Geometry

As stated above, the miss distance, *m*, is the quantity to be controlled. Therefore, *m*, is the control variable, *y*, see Equation (53).

$$y = m = R\sin(\chi_T - \chi) \tag{53}$$

The input to the dynamic inverter is the first derivative of the control variable, *y*. See Equation (55) and Figure 3-5.

$$\dot{y} = \frac{d}{dt}[R\sin(\chi_T - \chi)] \tag{54}$$

$$\dot{y} = \dot{R}\sin(\chi_T - \chi) + R\cos(\chi_T - \chi)(\dot{\chi}_T - \dot{\chi}) \tag{55}$$

Recalling from the equations of motion, See Equations (2) through (9), the heading control is,

$$\omega = \dot{\chi} \tag{56}$$

Solving Equation (55) for the control,

$$\dot{\chi} = \frac{-\dot{y}}{R\cos(\chi_T - \chi)} + \frac{\dot{R}\sin(\chi_T - \chi)}{R\cos(\chi_T - \chi)} + \frac{R\cos(\chi_T - \chi)}{R\cos(\chi_T - \chi)}\dot{\chi}_T \tag{57}$$

It can be shown that,

$$\frac{\dot{R}\sin(\chi_T - \chi)}{R\cos(\chi_T - \chi)} + \frac{R\cos(\chi_T - \chi)}{R\cos(\chi_T - \chi)}\dot{\chi}_T = 0 \tag{58}$$

Therefore the control, u, is expressed by,

$$u_{cmd} = \dot{\chi} = \frac{-\dot{y}_{des}}{R_{meas}\cos(\chi_T - \chi)} \tag{59}$$

For the feedback control systems developed here, the input to the dynamic inverter is defined as the difference between the commanded output and the actual output times a gain. See Figure 3-5 and Equation (60).

$$\dot{y}_{des} \equiv k_m(y_c - y) \tag{60}$$

$$\dot{y}_{des} = -k_m R \sin(\chi_T - \chi) \tag{61}$$

Equation (60) can be substituted into Equation (59), resulting in:

$$u_{cmd} = \frac{k_m R \sin(\chi_T - \chi)}{R \cos(\chi_T - \chi)} \tag{62}$$

$$u_{cmd} = k \tan(\chi_{Tmeas} - \chi_{meas}) \tag{63}$$

Equation (63) is the control law that was inserted into the heading control loop to steer the receiver to the waypoints. The next element of the heading control loop to be discussed is the geometric waypoint estimator, which will be referred to as the Dubins path generator.

The Dubins path generator uses the MATLAB scripts which were introduced in paragraph 3.2 and are described in more detail in Appendix A to generate an optimal path to the rendezvous condition. The Dubins path generator outputs two navigation waypoints along with the path distance and time to intercept. The first waypoint is the start of the second arc of the Dubins path and will be referred to as the predicted turn point. The second waypoint is the end of the second arc and will be referred to as the predicted intercept point. See Figure 3-7.

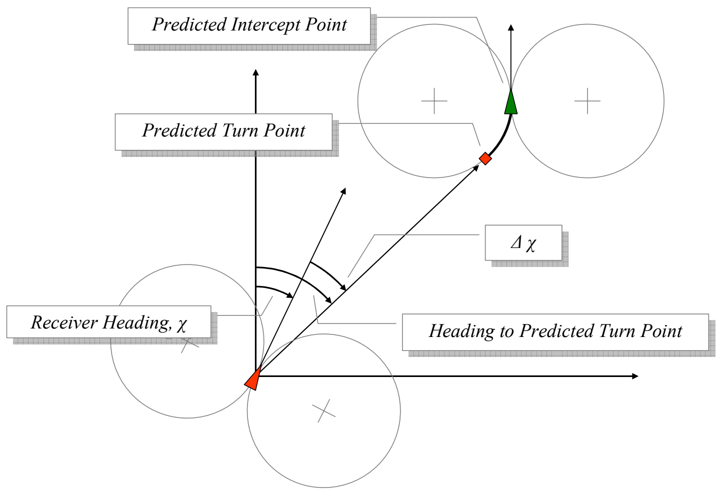

Figure 3-7 Predicted Turn Point And Predicted Intercept Point

Once the predicted turn point has been calculated, the dynamic inversion controller drives the receiver onto a heading that will intercept the predicted turn point (PTP). The control law is described by Equation (67). The tangent term in Equation (67) was derived by dynamic inversion and creates a non-linear effect that reduces the gain when the error is small to reduce jitter and increases the gain when the error is large to ensure saturation. The desired turn rate is then restricted by aircraft dynamics, modeled as a lowpass filter, $\frac{20}{S+20}$, and bounded by upper and lower constraints. See Table 2-2.

At each time step a new PTP is calculated, until, at a range of .15 turn radii to the predicted intercept point, the controller switches to the next waypoint, the predicted intercept point. The predicted intercept point at this time is held, i.e., not updated, until the receiver gets within .15 turn radii of the predicted intercept point, at which point, the simulation ends. A block diagram showing the heading controller can be found in Figure 3-8. A block diagram of the receiver model can be found in Figure 3-9.

$$p_{tgt} = \begin{cases} PTP & \text{while } |p_r - PTP| \geq 1.5 \\ PIP & \text{once } |p_r - PTP| < 1.5 \end{cases} \tag{64}$$

$$[\Delta n, \Delta e] = [p_{tgt}] - [p_r] \tag{65}$$

$$\chi_{des} = \arctan(\frac{\Delta n}{\Delta e}) \tag{66}$$

$$\Delta\chi = \chi_{des} - \chi, \text{ such that, } -\pi < \Delta\chi < \pi \tag{67}$$

$$\omega_{des} = k\tan(\Delta\chi / 2), \; where\ -\pi < \Delta\chi < \pi \tag{68}$$

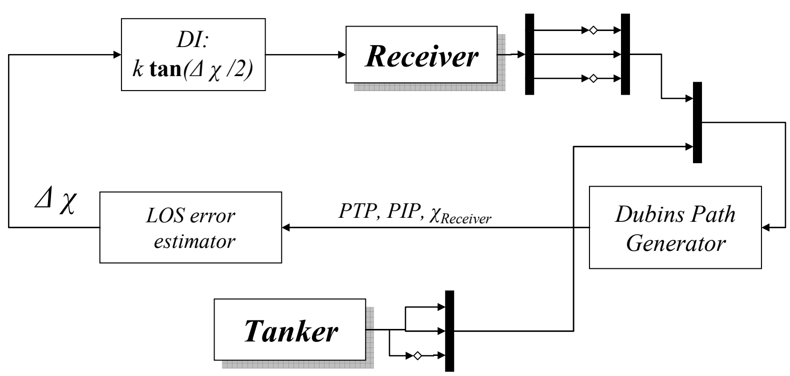

Figure 3-8 Heading Control Loop

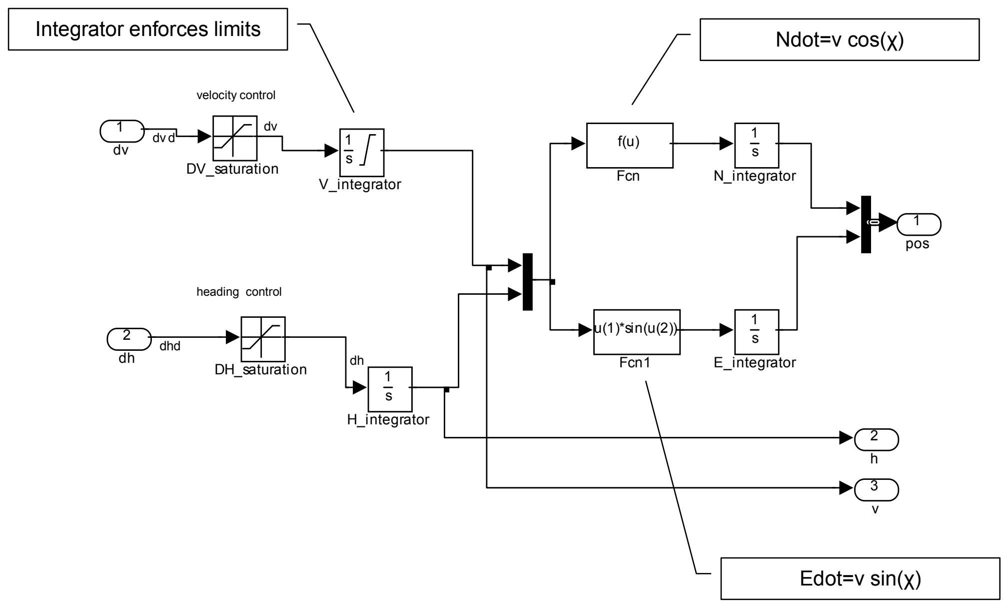

Figure 3-9 Receiver Model

Velocity Controller

The velocity controller has two modes. Since the objective of this controller is to arrive in the minimum time, the first mode accelerates the receiver to maximum speed. The second mode matches the speed of the receiver to the speed of the tanker. The modes switch at a fixed critical distance, D_C, from the predicted intercept point, based on the specific values for maximum airspeed and maximum deceleration. The minimum value of D_C is derived in Equation (75), below.

$$D_C = \int_0^T V(t)dt \tag{69}$$

$$V(t) = V_{\max} - a \cdot t \tag{70}$$

$$D_C = \int_0^T [V_{\max} - a \cdot t]dt \tag{71}$$

$$D_C = V_{\max} \cdot T - \frac{1}{2} a \cdot T^2 \tag{72}$$

$$T = \frac{V_{\max} - V_o}{a_{\min}} \tag{73}$$

$$D_C = V_{\max} \cdot \frac{V_{\max} - V_o}{a_{\min}} - \frac{1}{2} a \cdot (\frac{V_{\max} - V_o}{a_{\min}})^2 \tag{74}$$

$$D_C = \frac{V_{\max}^2 - V_o^2}{2a} \tag{75}$$

The velocity control law is given by Equation (77). Outside of D_C, the commanded acceleration is a fixed value resulting in maximum acceleration until the maximum velocity is achieved. Once the receiver is inside D_C the control law changes to match the velocity of the tanker, the signed square of the velocity difference used to quickly drive the receiver velocity close to the velocity of the tanker. It is not necessary that velocities match exactly; therefore, the flattening of the parabola in the neighborhood of zero is acceptable. To approximate reality, all desired acceleration commands are bounded by upper and lower

constraints. See Equation (76) for implementation and Table 2-2 for values. Figure 3-10 shows a block diagram showing the velocity controller.

$$a = \begin{cases} a_{\min} & \text{if } a_{des} \le a_{\min} \\ a_{des} & \text{if } a_{\min} < a_{des} < a_{\max} \\ a_{\max} & \text{if } a_{des} \ge a_{\max n} \end{cases} \tag{76}$$

Where,

$$a_{desired} = \begin{cases} .1 & \text{if } D > D_C \\ k \times \Delta \mathrm{v} \times |\Delta \mathrm{v}| & \text{if } D \le D_C \end{cases} \tag{77}$$
$$\text{where, } k = 10$$

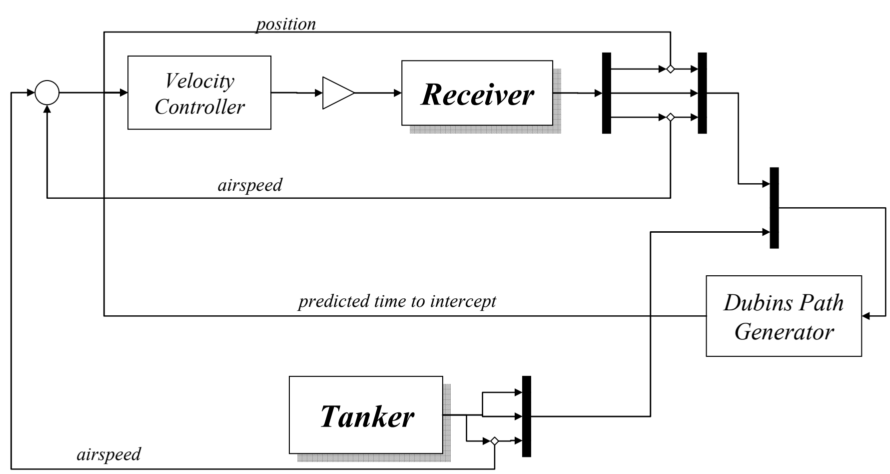

Figure 3-10 Velocity Control Loop

3.3.2. Specified Time Controller

The specified time controller will generate heading rate and acceleration commands to achieve a rendezvous at a specified time. It accomplishes this by the use of two control loops: a heading control loop a time of arrival control loop. The heading control loop is similar to that of the minimum time controller. The time of arrival controller performs similarly to the minimum time controller's velocity control loop, but also produces commands that limit the allowable turn rate.

Heading Controller

The heading controller for the specified arrival time problem is identical to the heading controller for the minimum time problem, with the exception of the fact that the radius of the Dubins path arcs are allowed to vary based on inputs from the velocity controller. It should also be noted that because the turn rates are limited by the time of arrival controller, the two control loops become closely coupled. See Figure 3-11 and Figure 3-12.

$$\varepsilon_{ARRIVAL} = ETA - RTA \tag{78}$$

$$\frac{d\omega}{dt} = k(\varepsilon_{ARRIVAL}) \tag{79}$$

$$|\omega_{\max}| = \int_{t_0}^{T} \frac{d\omega}{dt} dt \tag{80}$$

Since the specified time controller can restrict the turn rate, the gain must be smaller in this controller so that there still exists a range of $\Delta\,\chi$s that do not saturate the turn rate. To achieve this, the gain was reduced from 10 to 5. Ideally, this gain would vary as a function of maximum turn rate.

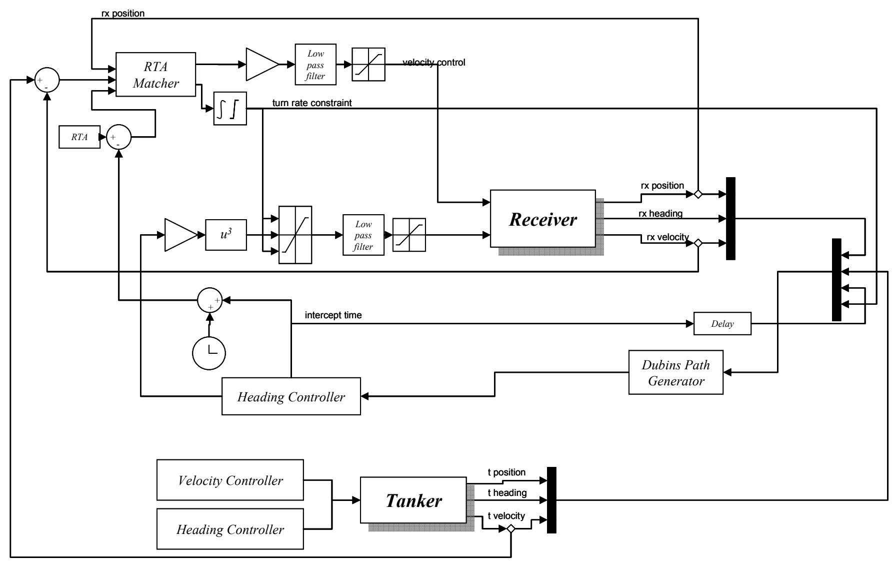

Figure 3-11 Specified Time Controller

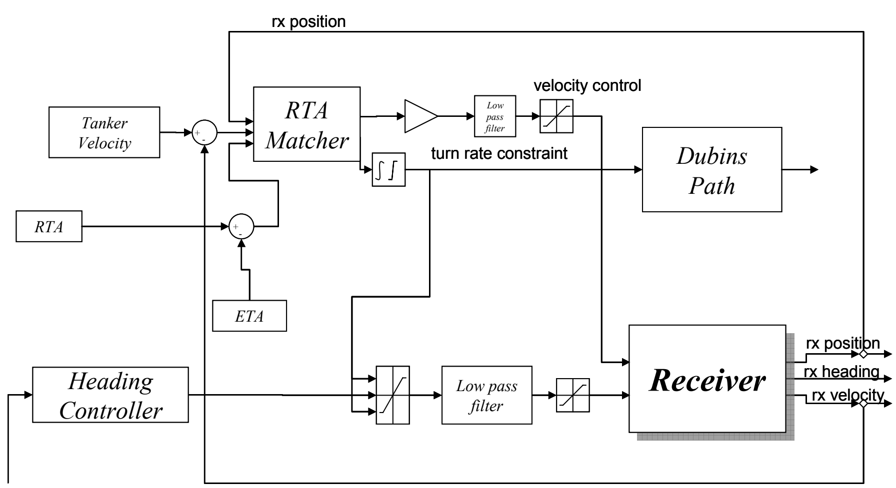

Figure 3-12 Specified Time Controller (Detail)

Time of Arrival Controller

The time of arrival controller has three modes. The first two modes, Late Mode and Early Mode attempt to achieve a rendezvous at the desired time. In addition to the controlling speed, the velocity controller also sends a signal to the Dubins routine to increase the radius of the Dubins path arc. The desired effects and control laws for all three modes are contained in Table 3-1. The third mode matches the speed of the receiver to the speed of the tanker. The modes switch at a fixed distance, D_C, from the predicted intercept point, based on the specific values for maximum airspeed and maximum deceleration. The value of D_C is derived in Equation (75), above.

Table 3-1 Specified Time Control Laws

Mode	Late	Early	Terminal
RTA-ETA:	-	+	Either
Desired Effect on Radius	Decrease	Increase	Either
Desired Effect on Turn Rate	Increase	Decrease	Either
Desired Acceleration	Increase if necessary, else, match tanker	Match tanker	Match Tanker
$\dot{\omega}$	$-\frac{\varepsilon_{Arrival}}{30}+3\times\varepsilon_{Velocity}^{2}$	$-\frac{\varepsilon_{Arrival}}{30}$	$-\frac{\varepsilon_{Arrival}}{20}$
	Note: If Arrival Error is small, then the Velocity Error dominates. Therefore, if the receiver is fast, the turn radius is restricted, which results in the receiver being early, which results in a negative acceleration command.		
a	$-\varepsilon_{Arrival}^{2}+.02\times\varepsilon_{Velocity}\times\left\|\varepsilon_{Velocity}\right\|$	$4\times\varepsilon_{Velocity}\times\left\|\varepsilon_{Velocity}\right\|$	$4\times\varepsilon_{Velocity}\times\left\|\varepsilon_{Velocity}\right\|$

3.4. Dynamic Optimization

Numeric dynamic optimization is used as a comparison for the results of the feedback controller simulation. The numeric optimization function that will be used is *fmincon*, which is part of the MATLAB optimization toolbox. Since *fmincon* is a parameter optimization tool, the problem will be discretized as described on above. The dynamic optimization routine is passed the receiver initial state, the desired intercept state, an estimated intercept time, and an initial guess of the required control. Since *fmincon* requires an accurate initial guess, the estimated intercept time and the control guess are generated from the Dubins path.

Dynamic optimization will be used to calculate the optimal heading control required to get from the initial state to the rendezvous point.

Since the final time is free, it is convenient to fix the number of discrete time steps and allow the length of the time steps to vary, so that the discretization of time can be expressed by Equation (81).

$$t_f = t_0 + N\Delta t \text{, where } N\text{=the number of time steps} \tag{81}$$

$$t_i = t_0 + i\Delta t \tag{82}$$

The discrete state and control vectors are represented by Equations (83) and (84).

$$S(i)=\begin{Bmatrix} N_R \\ E_R \\ \chi_R \\ V_R \end{Bmatrix} \tag{83}$$

$$U(i)=\begin{Bmatrix} \omega(i) \\ a(i) \end{Bmatrix} \tag{84}$$

Euler's integration technique was used to propagate the state equations, Equation (5) forward in time. The discrete state equations are now represented by Equation (85).

$$S(i+1)=f(S(i),U(i),\Delta T)=\begin{Bmatrix} x(i+1) \\ y(i+1) \\ \chi(i+1) \\ v(i+1) \end{Bmatrix}=\begin{Bmatrix} x(i)+\dot{x}(i)\Delta T \\ y(i)+\dot{y}(i)\Delta T \\ \chi(i)+\dot{\chi}(i)\Delta T \\ v(i)+\dot{v}(i)\Delta T \end{Bmatrix} \tag{85}$$

where *i=0, 1 ,2,…N-1*

In this problem, both the controls and the states are bounded. The constraints on the controls are expressed in Equation (86).

$$\begin{aligned} a_{\min} &\le a \le a_{\max} \\ \omega_{\min} &\le \omega \le \omega_{\max} \end{aligned} \tag{86}$$

Terminal constraints are used to enforce the required rendezvous conditions; specifically, the receiver must have the same position, heading, and airspeed as the tanker.

$$\psi = \begin{Bmatrix} x_r(t_f) - x_t(t_f) \\ y_r(t_f) - y_t(t_f) \\ \chi_r(t_f) - \chi_t(t_f) \\ v_r(t_f) - v_t(t_f) \end{Bmatrix} = \{0\} \tag{87}$$

3.4.1. Minimum Time Problem Setup

The intent of this problem is to create a series of control inputs that drive the receiver to arrive at the rendezvous point (1 nm behind the tanker) at the same time, while matching air speed and heading, in minimum time, subject to the dynamic constraints of the vehicle. This problem can be expressed either with terminal constraints or with the desired terminal conditions included in the cost function. Through trial and error, it has been found that in this case, the combination of firm constraints with the constraints added to the cost function results in more robust solutions and faster convergence times. Additionally, by including the constraints in the cost the feedback controller can be directly compared to the results of the optimization by applying the same cost function. The final dynamic optimization problem for the minimum time rendezvous problem was:

Minimize:

$$
\begin{gathered}
J = \phi + \int_{t_0}^{t_f} L dt \\
\text{where, } \phi = t + x_f Q x_f \\
\text{where, } Q = \begin{bmatrix} 1 & 0 & 0 & 0 \\ 0 & 1 & 0 & 0 \\ 0 & 0 & 50 & 0 \\ 0 & 0 & 0 & 1 \end{bmatrix} \\
\text{and } x_f = \begin{bmatrix} y_{rf} - y_{tf} \\ x_{rf} - x_{tf} \\ \chi_{rf} - \chi_{tf} \\ v_{rf} - v_{tf} \end{bmatrix} \\
\text{and where } L = u(t)^T R u(t) \\
\text{where } u = \begin{bmatrix} \overline{\omega} & \overline{a} \end{bmatrix}^T \\
\text{and R=} \begin{bmatrix} 1 & 0 \\ 0 & 30 \end{bmatrix}
\end{gathered}
\tag{88}
$$

Subject to:

Terminal Constraints:

$$N_{R_f} = N_{T_f} \tag{89}$$

$$E_{R_f} = E_{T_f} \tag{90}$$

$$\chi_{R_f} = \chi_{T_f} \tag{91}$$

$$V_{R_f} = V_{T_f} \tag{92}$$

Control and State Constraints:

$$|\omega| \leq \dot{\chi}_{\max} \tag{93}$$

$$\dot{V}_{\min} \leq a \leq \dot{V}_{\max} \tag{94}$$

$$V_{\min} \leq V \leq V_{\max} \tag{95}$$

3.4.2. Specified Time Problem Setup

The intent of this problem is to create a series of control inputs that drive the receiver to arrive at the rendezvous point (1 nm behind the tanker), while matching air speed and heading, at a specified time, subject to the dynamic constraints of the vehicle. Again, this problem can be expressed either with terminal constraints or with the desired terminal conditions included in the cost function. Through trial and error, it has been found that in this case, the combination of firm constraints with the constraints in the cost function results in more robust solutions and faster convergence times.

Cost function and constraints

The final dynamic optimization problem for the specified rendezvous problem was:

Minimize:

$$
\begin{aligned}
&J = \phi + \int_{t_0}^{t_f} L dt \\
&\text{where, } \phi = RTA - t + x_f Q x_f \\
&\text{where, } Q = \begin{bmatrix} 1 & 0 & 0 & 0 \\ 0 & 1 & 0 & 0 \\ 0 & 0 & 50 & 0 \\ 0 & 0 & 0 & 1 \end{bmatrix} \\
&\text{and } x_f = \begin{bmatrix} y_{rf} - y_{tf} \\ x_{rf} - x_{tf} \\ \chi_{rf} - \chi_{tf} \\ v_{rf} - v_{tf} \end{bmatrix} \\
&\text{and where } L = u(t)^T R u(t) \\
&\text{where } u = \begin{bmatrix} \overline{\varpi} & \overline{a} \end{bmatrix}^T \\
&\text{and R=} \begin{bmatrix} 1 & 0 \\ 0 & 30 \end{bmatrix}
\end{aligned}
\tag{96}
$$

Subject to:

Terminal Constraints:

$$N_{R_f} = N_{T_f} \tag{97}$$

$$E_{R_f} = E_{T_f} \tag{98}$$

$$\chi_{R_f} = \chi_{T_f} \tag{99}$$

$$V_{R_f} = V_{T_f} \tag{100}$$

Control and State Constraints:

$$|\omega| \le \dot{\chi}_{\max} \tag{101}$$

$$\dot{V}_{\min} \le a \le \dot{V}_{\max} \tag{102}$$

$$V_{\min} \le V \le V_{\max} \tag{103}$$

3.5. Summary

Two problems are being considered. The first is rendezvousing with a tanker in the shortest period of time. The second is rendezvousing with a tanker at a specified time. In either case, the receiver must match speed and heading with the tanker.

4. Results and Discussion

4.1. Chapter Overview

This chapter presents and analyzes the results of the simulation and dynamic optimization. First the results from the minimum time problem are presented, followed by the results from the fixed final time problem.

4.2. Minimum Time Problem

In this section, results from the minimum time problem simulation and dynamic optimization are presented, analyzed, and compared.

4.2.1. Rendezvous Controller

In this section, results from an individual case will be presented to demonstrate in detail the results and then the results from multiple cases will be presented.

Case 1: E=10, N=8, χ= 0, V_o=1.2

This case is presented in detail as an example of the minimum time controller. For this case, the receiver starts ahead of and to the right of the tanker, headed parallel to and in the same direction as the tanker's path of flight. The receiver starts off making maximum acceleration; since it is already at maximum speed this has no effect. It also starts off making a minimum radius left turn toward the predicted turn point. During this maneuver, at time=1.7 (recall, this is a normalized time), the velocity controller switches mode to begin matching speed with the tanker. As the speed of the receiver begins to decrease, the predicted turn point begins to move down range (North). Once the receiver rolls out of the minimum radius left turn, at time=2.2, the receiver enters a very mild right hand turn as it

tracks the slowly moving predicted intercept point. Once the receiver passes within .15 radii of the current predicted turn point, it holds the current predicted intercept point and enters a minimum radius right hand turn toward the predicted intercept point. As it homes in on the tanker, the receiver overshoots slightly, makes a slight heading correction, which can be seen in Figure 4-1.

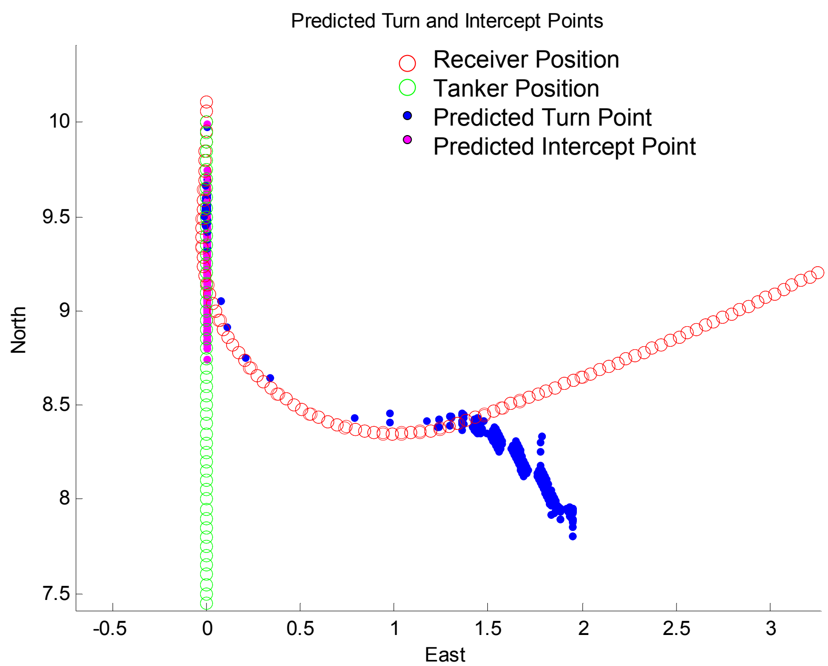

Figure 4-1 Rendezvous Endgame

By observation, the path taken by the receiver can be seen to be approximately a Dubins path. More importantly, the turn rate commands also approximate those expected from a CLC Dubins path; that is, “bang-zero-bang”. This can be seen in the Heading Control Plot of Figure 4-2. Likewise, the velocity commands go from maximum acceleration to maximum deceleration. Since the objective is to rendezvous in minimum time and to match speed, this “bang-bang” control approximates the optimal control. This can be seen in the Velocity Control Plot of Figure 4-2. Two things should be noted about

the velocity control. First, the mode switches prior to the critical distance discussed on page 38 and expressed in Equation (75). Second, the gain is low enough that the deceleration command trails off rather than being saturated until it drops off straight to zero. The mode switches prior to the critical distance for two reasons: the first is so that the geometry will not be rapidly changing in the end game; the second is to allow for the velocity to trail off while still matching the tanker velocity. The reason the gain is low enough that the acceleration command becomes unsaturated, is to avoid instability associated with high gain, particularly large oscillations in velocity. Additionally, it should be noted that at time=9.1, the velocity controller reverts to maximum acceleration mode. This is because as the range to the tanker becomes small and if the receiver is not exactly on the desired course, the Dubins algorithm projects that a long Dubins path is required to get the receiver to properly intercept. Because of the long Dubins path, the receiver is now no longer in the critical distance of the intercept turn point and the velocity controller reverts to maximum acceleration mode. In the final implementation, this would be avoided, since the algorithm would terminate once the headings, positions, and airspeed match within the required tolerance.

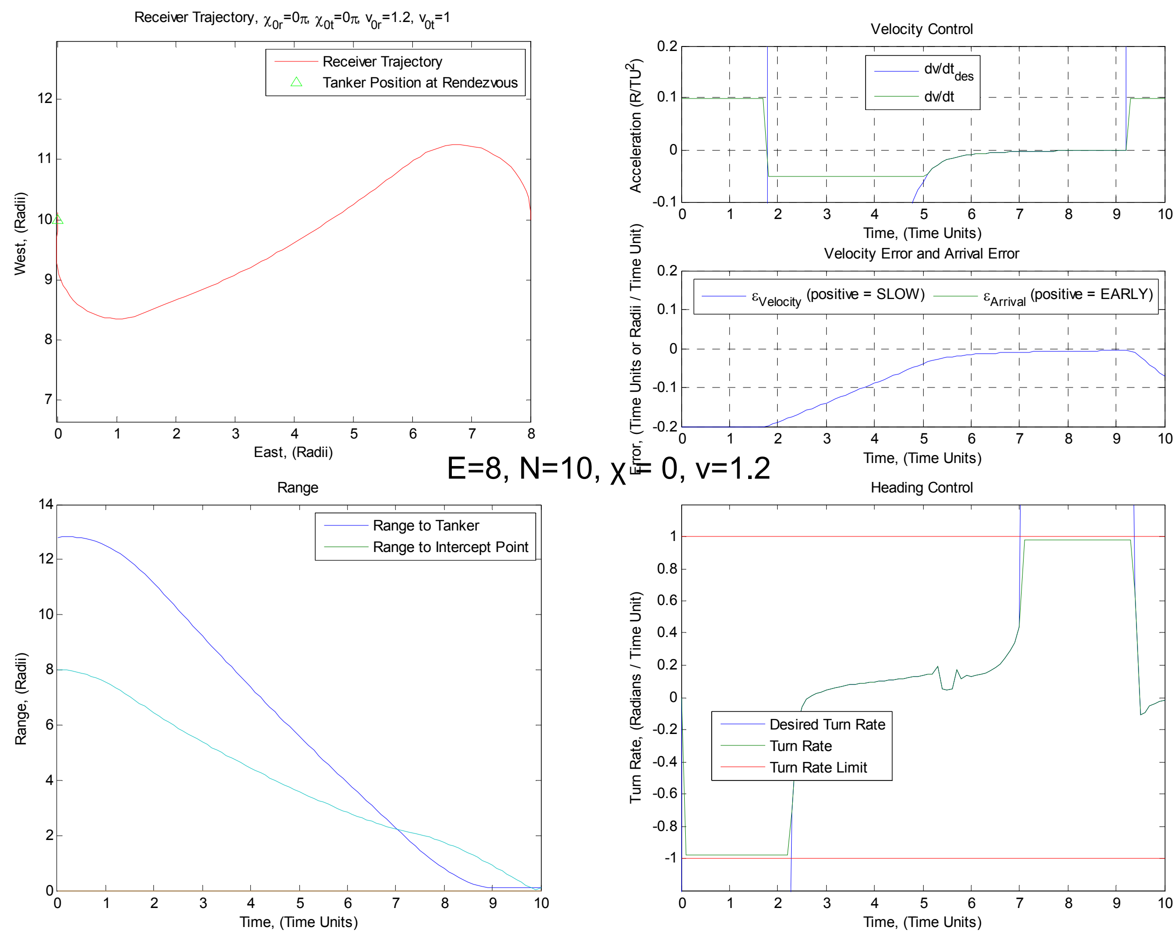

Figure 4-2 Plots from E=10, N=8, χ = 270 deg, v_0=1.2

Multiple cases

The purpose of this section is to demonstrate the robustness of the controller and areas where it has difficulties. There are four things that should be observed from these results. First, it should be noted that the plot of the rendezvous times as a function of receiver initial position is mostly smooth. See Figure 4-3. Second, it should be noted that the rendezvous times are higher when the receiver starts near the tanker trajectory; this is unexpected and will be examined further. Thirdly, when the receiver starts near the tanker's trajectory and with little down range separation, the rendezvous time is much higher. This is

expected due to the assumption violation. Lastly, rendezvous times begin to increase more rapidly than expected when down track separation is small, but cross track separation is large.

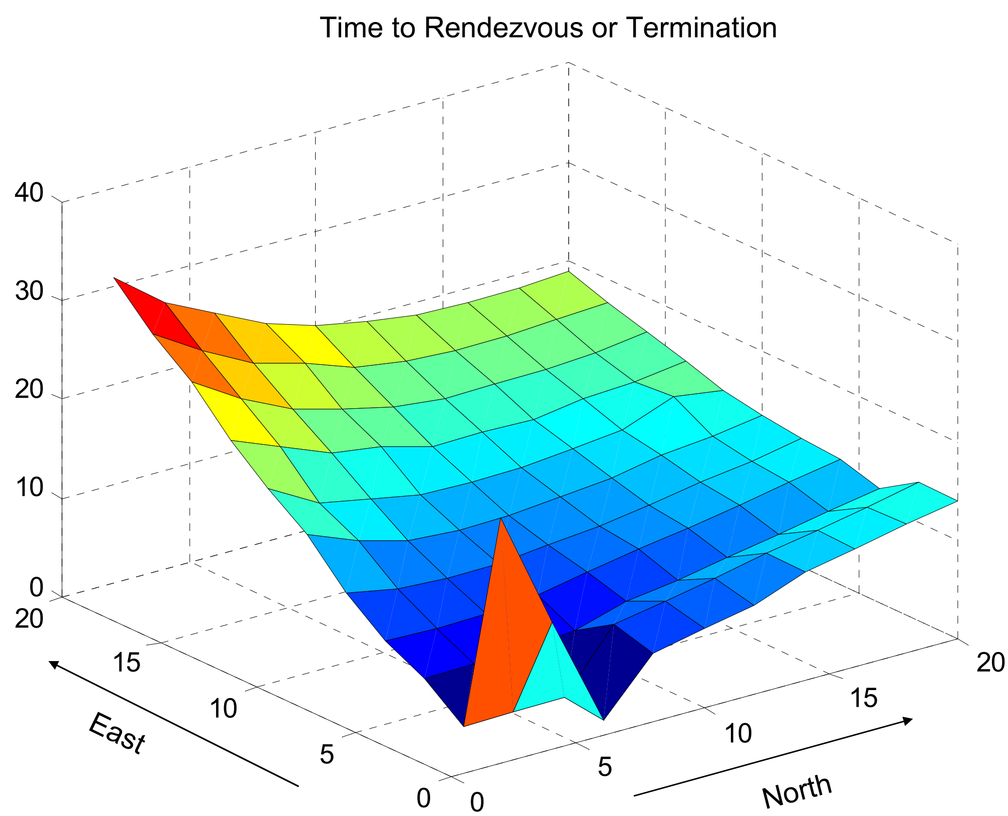

Figure 4-3 Dubins Controller Rendezvous Times for V_0=1.2, χ_0 = 0

As pointed out above, for a large region of initial conditions, the controller is able to effect a successful rendezvous. When the cross track offset is greater than four turn radii and less than roughly four times the down track, the controller is very well behaved. By inspection, the trajectories approximate Dubins paths and the terminal conditions are met.

One of the most challenging scenarios for autonomous rendezvous involves the receiver and tanker heading towards each other: traditional missile-guidance-type controllers would drive the aircraft to a head-on collision. Unfortunately, at this time, while

the Dubins controller does not produce a collision, it is unable to successfully rendezvous when the receiver is in front of the tanker, in a corridor four turn radii on either side of the tanker's trajectory, and with an arbitrary heading. When the heading is limited to the opposite direction of the tanker, the corridor can be limited to two turn radii on either side of the tankers trajectory. See Figure 4-6. This is due to the geometry breakdown when the assumption of four radii separation is violated. It may be possible to develop an additional controller that will help the receiver to egress this corridor and achieve a successful rendezvous.

When the cross track initial position is greater than roughly four times the down track initial position (see Figure 4-9), the controller currently runs into an additional problem. Since the receiver is chasing the tanker, the intercept point is extremely dependent on the velocity difference between the receiver and the tanker. When the velocity controller changes modes the intercept point begins to drift down range, causing the receiver to make a gradual (non-optimal) turn toward the new intercept point.

This was fixed by using an estimator to predict the future average velocity of the receiver up to intercept. Prior to velocity mode change the estimated average velocity is calculated using Equation (104), the weighted average of the current velocity and the calculated average velocity during the deceleration. After the velocity mode change, the average velocity is estimated by Equation (105), the average of the current velocity and the rendezvous velocity. The trajectories of the receiver using this estimator are shown in Figure 4-7 and Figure 4-8.

$$v_{avg} \approx v_{fast} \times \frac{T_{fast}}{T_{tot}} + v_{slow} \times \frac{T_{slow}}{T_{tot}}$$

where $T_{fast} = T_{tot} - T_{slow}$

T_{tot} is the estimated time to intercept (104)

T_{slow} is the estimated time required to decelerate

v_{fast} is the current airspeed

v_{slow} is the average speed during deceleration

$$v_{avg} \approx \frac{v(t) + v_{rendezvous}}{2}$$

where:

T_{tot} is the estimated time to intercept (105)

T_{slow} is the estimated time required to decelerate

$v(t)$ is the current airspeed

$v_{rendezvous}$ is the desired rendezvous airspeed

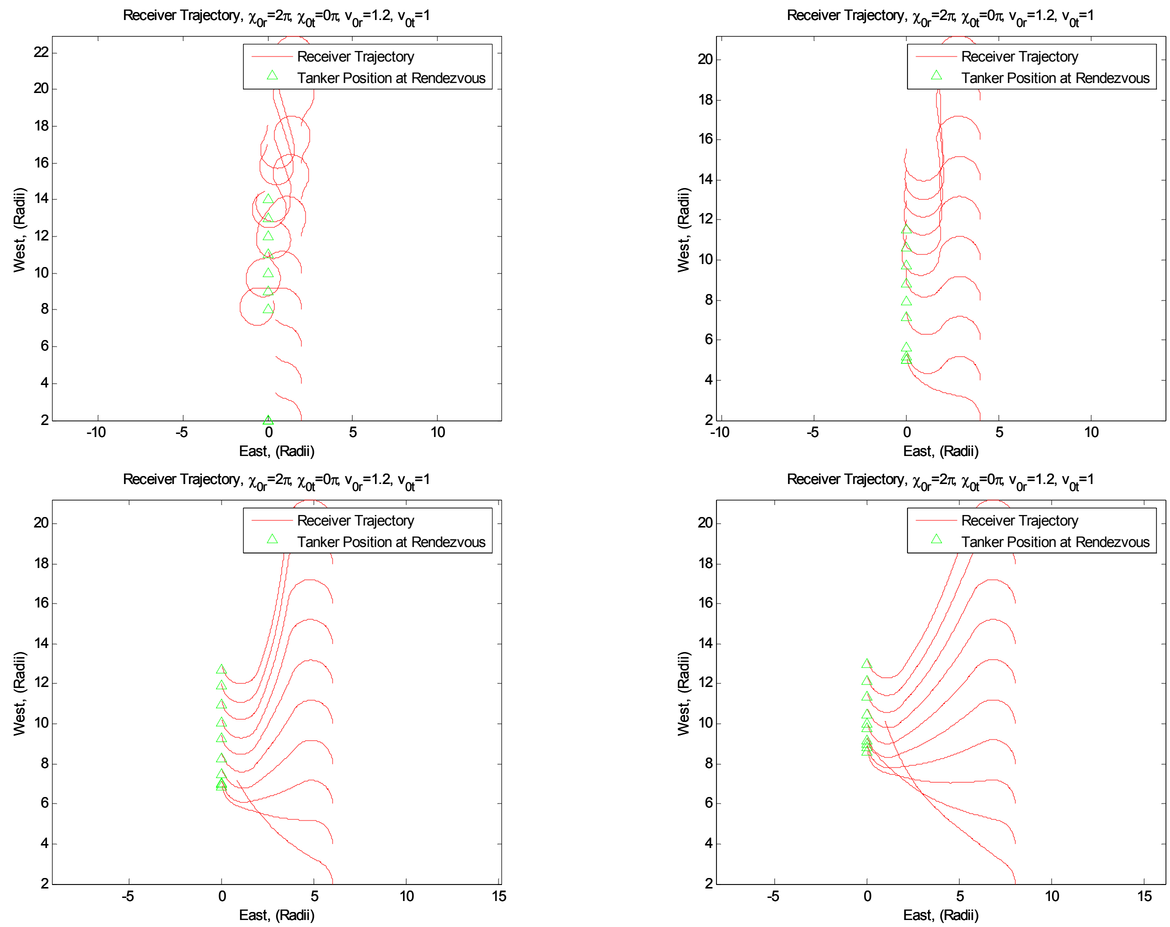

Figure 4-4 Trajectories for cross track=2 through 6

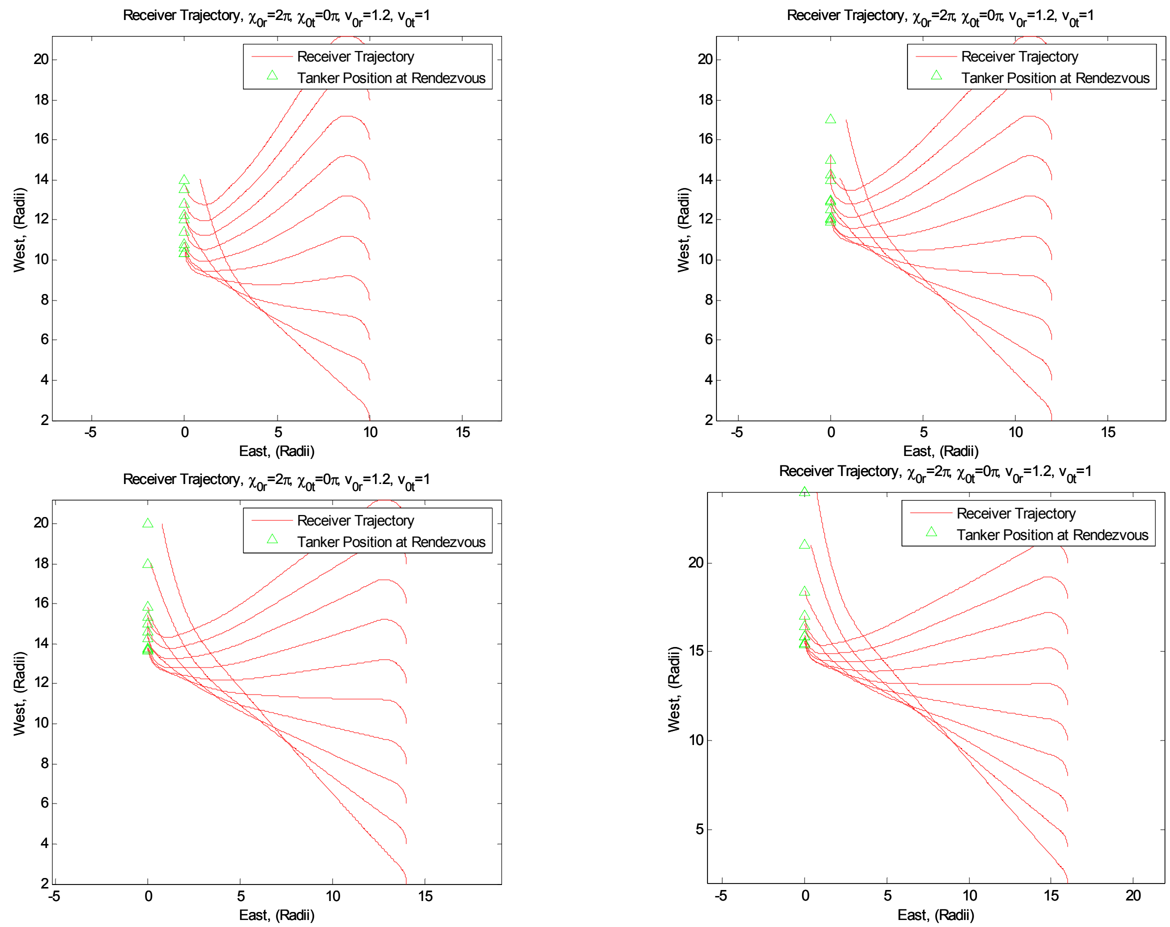

Figure 4-5 Trajectories for cross track =8 throught 16

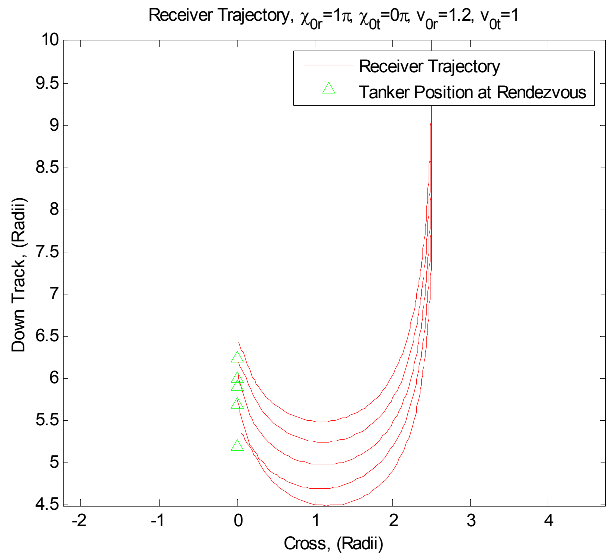

Figure 4-6 Well-behaved Trajectories at an offset of 2.25 radii

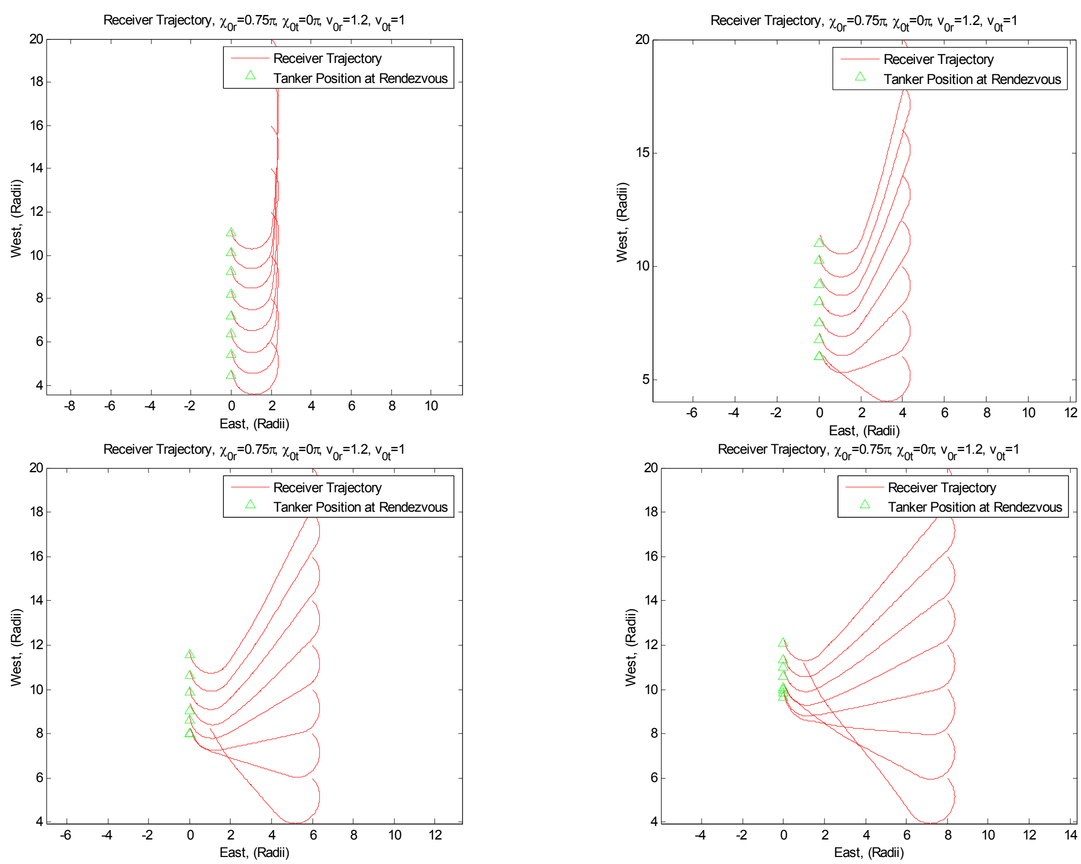

Figure 4-7 Trajectories with Estimator, Cross Track = 2 through 8

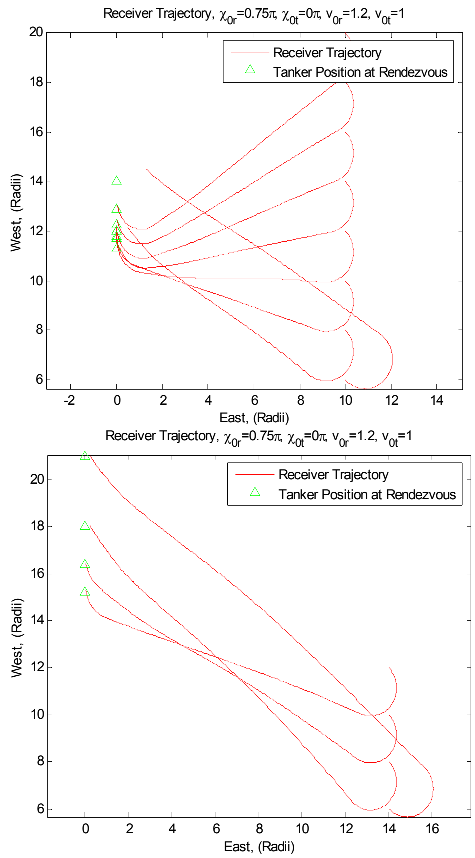

Figure 4-8 Trajectories with Estimator, Cross Track = 10 through 14

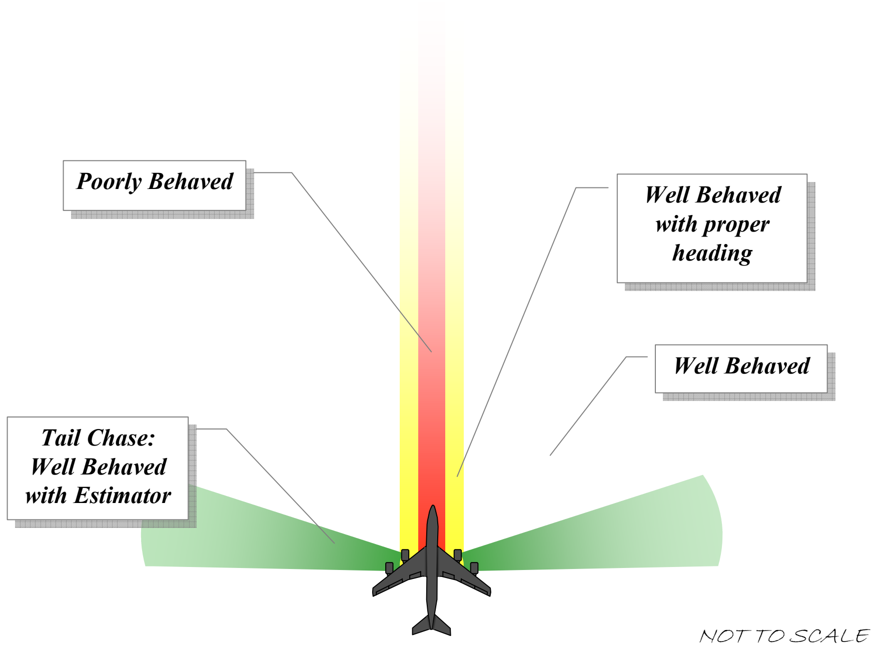

Figure 4-9 Regions of Behavior

4.2.2. Dynamic Optimization

<u>*Single case*</u>

This case is presented in detail to provide insight into the dynamic optimization results. For this case, the tanker starts ahead of and to the right of the tanker, headed parallel to and in the same direction as the tanker's path of flight. See Figure 4-10. As predicted by L.E. Dubins [Dubins 1957], the trajectory of the constant velocity case appears to consist of minimum radius turns and straight line segments. This is confirmed by examining the turn rates. With a few exceptions, the "optimal" control follows the expected maximum turn rate, zero turn rate, maximum turn rate.

When velocity is allowed to vary, there is very little difference in the trajectory; however, there is an observable difference in the heading commands. In the free velocity case, the heading commands are smoother, resulting in a slightly longer trajectory. The acceleration commands behave as expected; they exhibit bang-bang type control. See Figure 4-11. If the linear quadratic costs are increased, the heading commands become even smoother.

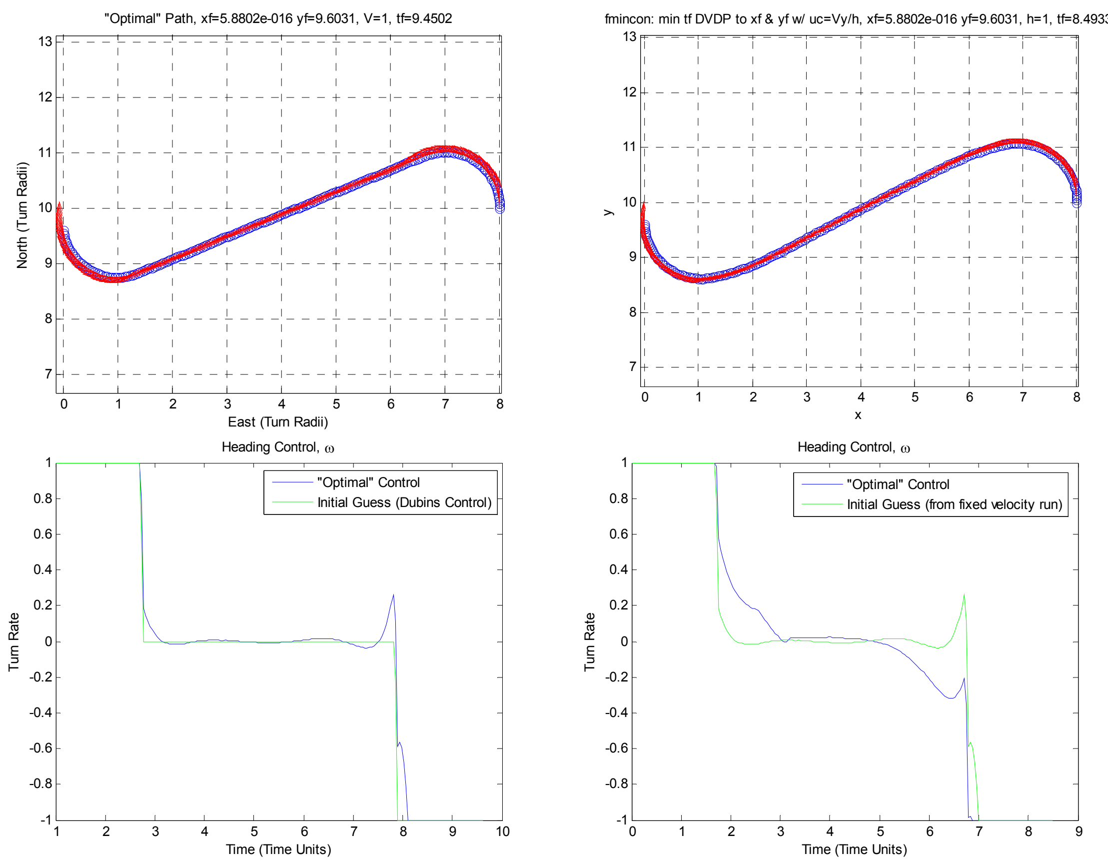

Figure 4-10 Optimal Trajectories and Heading Controls

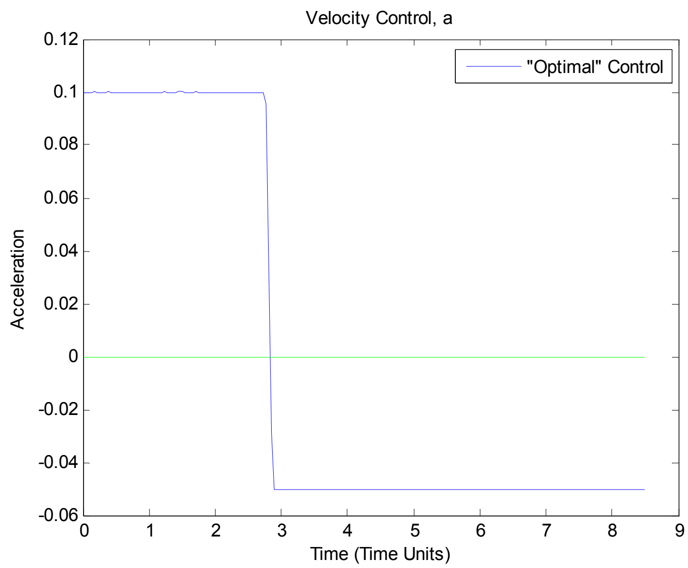

Figure 4-11 Velocity Control

Multiple cases

Multiple runs were conducted in two ways. The first was to vary the initial heading while keeping the initial position constant; the second was to keep the initial heading constant while varying the initial position in both cross track and down track position.

When the initial heading was varied, the heading histories for each initial heading were captured. The sine and cosine of these histories where plotted to create a surface. See Figure 4-12. In Figure 4-12, it can be seen that the initial heading was varied through 0-2π radians. By following the time axis, in every case the receiver rapidly turned in a direction toward the rendezvous point. It then maintained this heading until it neared the rendezvous point at which point it rapidly transitioned to the required terminal heading, in this case, zero. This demonstrates that for this initial position, the optimization technique was smooth for all headings.

When initial position was varied, the time to rendezvous was plotted as a surface, with the initial position as the independent variables. It can be seen that there is a region where the optimization technique produces smooth results and two regions where the results are not smooth. Coincidentally, these regions are approximately the same regions where the rendezvous controller is less successful. However, the usual failure mode for the dynamic optimization is to add additional loops to the trajectory. This can be seen in Figure 4-13, by observing that many of the peaks have approximately the same height. It should also be noted that in five cases (two are easily seen), the procedure fails outright and calculates rendezvous times below the plane of the surface, indicating that these instances are outliers that failed to meet the boundary conditions.

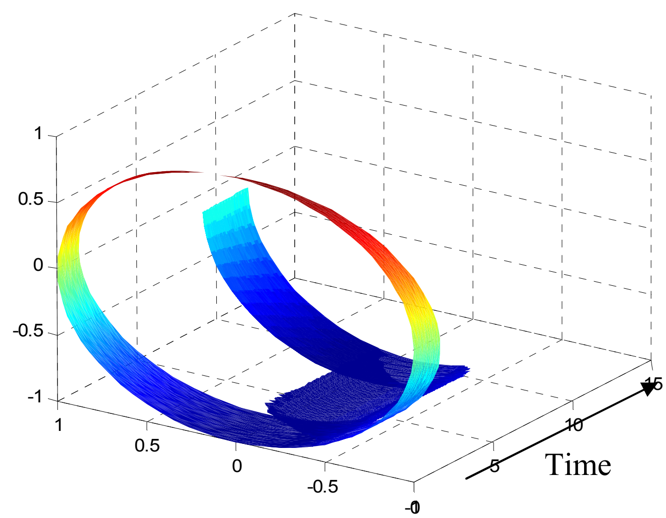

Figure 4-12 Optimal Headings, Varying Initial Heading

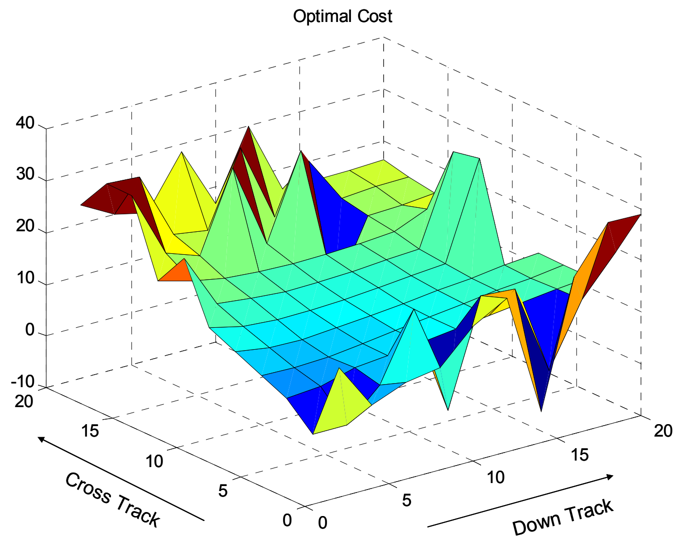

Figure 4-13 Rendezvous Times, Varying Initial Position

4.2.3. Comparison

Both the individual cases and the multiple cases will be compared.

Single Case

When comparing the optimal and Dubins trajectories, (see Figure 4-14), both have the same basic shape. The Dubins trajectory has a slight right hand curve during the straight portion, which will increase the time to rendezvous. This is likely caused by the change in the velocity affecting the projected turn point. The heading command histories also have the same basic shape. Again it is noted that the dynamic optimization heading commands where velocity is allowed to vary are less defined than for the fixed velocity case, but both have the expected shape and compare to the Dubins controller. By examining the rendezvous times additional insight can be gained about the performance. See Table 4-1. The rendezvous times for the Dubins controller and the velocity fixed optimization differ by about three

percent. However, the Dubins controller differs from the free velocity optimization by 14%. Since the difference in the paths cannot account for the difference,

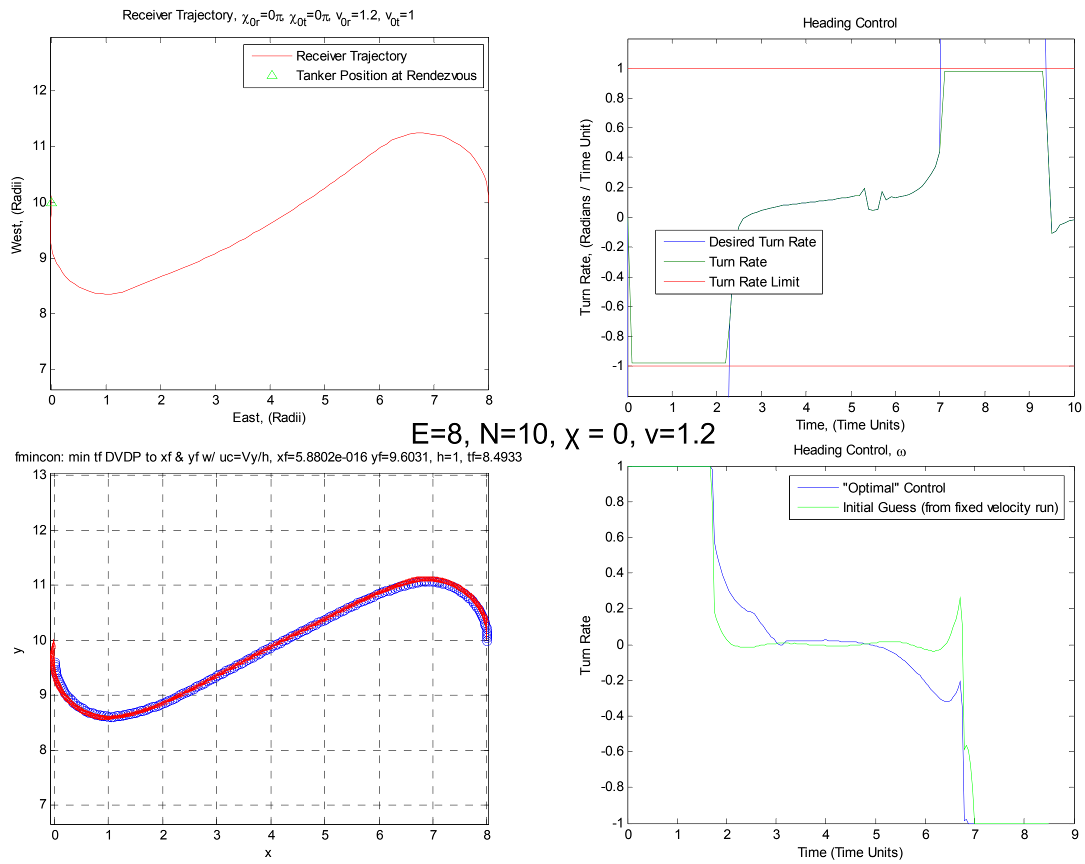

Figure 4-14 Optimal and Dubins Trajectories and Heading Commands

Table 4-1 Rendezvous Times

	Final Time	Percent of Optimal with Varying V
Dubins Controller	9.7	114%
Optimization, Constant V	9.45	111%
Optimization, Varying V	8.49	100%

Multiple Cases

A surface plot showing the difference between the rendezvous times using the rendezvous controller and the rendezvous times generated by dynamic optimization has been created. See Figure 4-15. This plot shows when both methodologies work properly, they are in close agreement.

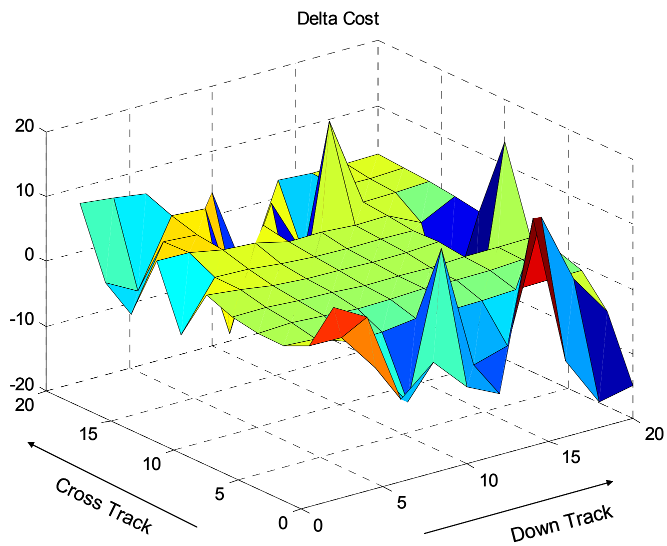

Figure 4-15 Difference between controller and optimal

4.3. Specified Time Problem

In this section, results from the specified time problem simulation and dynamic optimization are presented, analyzed, and compared.

4.3.1. Rendezvous Controller

In this section, results from an individual case will be presented to demonstrate in detail the results and then the results from multiple cases will be presented.

Single Case

This case is presented in detail as an example of the specified time controller. For this case, the receiver starts ahead of and to the right of the tanker, headed parallel to and in the same direction as the tanker's path of flight. As noted above, for the specified time problem, the turn rate is initially limited to .4 radians per time unit to help speed convergence to the correct turn rate. The receiver starts off making maximum acceleration because it is initially late. After time=1.2, the receiver is no longer late (due to the rapid increase in turn authority), however, the velocity control remains positive because of the lowpass filter. From time=1.2 to time=6.0, the positive (early) arrival error is driven down by a slight decrease in turn rate authority. Starting at t=6, the lowpass filter allows the velocity control to decay, change signs, and saturate to maximum deceleration. This deceleration causes the restriction on the turn rate to relax. At this point, the turn rate restriction is attempting to drive the arrival error to zero, while the acceleration command is attempting to drive the velocity error to zero. It should be noted that despite the estimated time of arrival of 20.1, the receiver still meets the rendezvous conditions at the required time of arrival.

Again, by observation, the path taken by the receiver can be seen to be approximately a Dubins path, however, in this case, it can be seen that the first turn has a much larger radius than the second. Ideally, the receiver should have begun slowing and decreasing turn rate authority sooner. However, the turn rate exhibits the expected CLC Dubins path of max-turn-rate, zero turn-rate, max-turn-rate. See Figure 4-16

Heading Control and the velocity control exhibits the desired “bang-bang” control and, most importantly the terminal conditions, position, v and χ, are satisfied. See Figure 4-16.

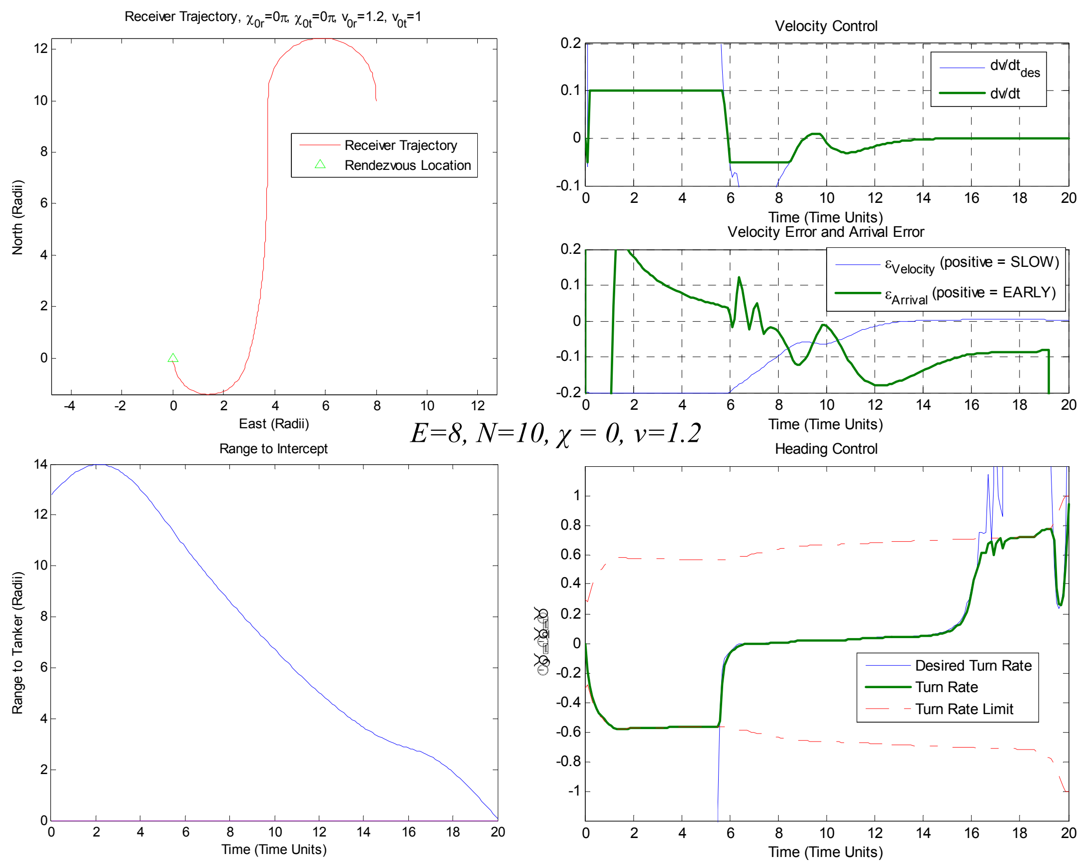

Figure 4-16 Specified Time Results for Single Case

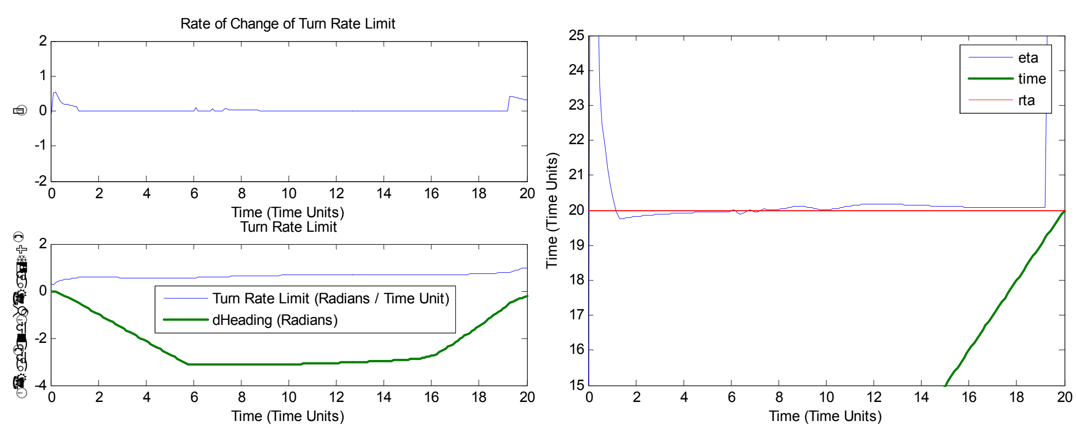

Figure 4-17 Turn Rate Limits and ETA

Multiple Cases

The purpose of this section is to demonstrate the robustness of the controller and identify areas where is has difficulties. Since the final rendezvous point is known and since the algorithm attempts to drive the velocity to the rendezvous velocity as early as possible, the Dubins controller does not run into the moving target problem experienced in the minimum time case. The biggest problem experienced by the Dubins controller was when the RTA was large enough to cause the turn circles to overlap or if there was not sufficient time to allow the turn radius constraint to reach the required value. See Figure 4-18.

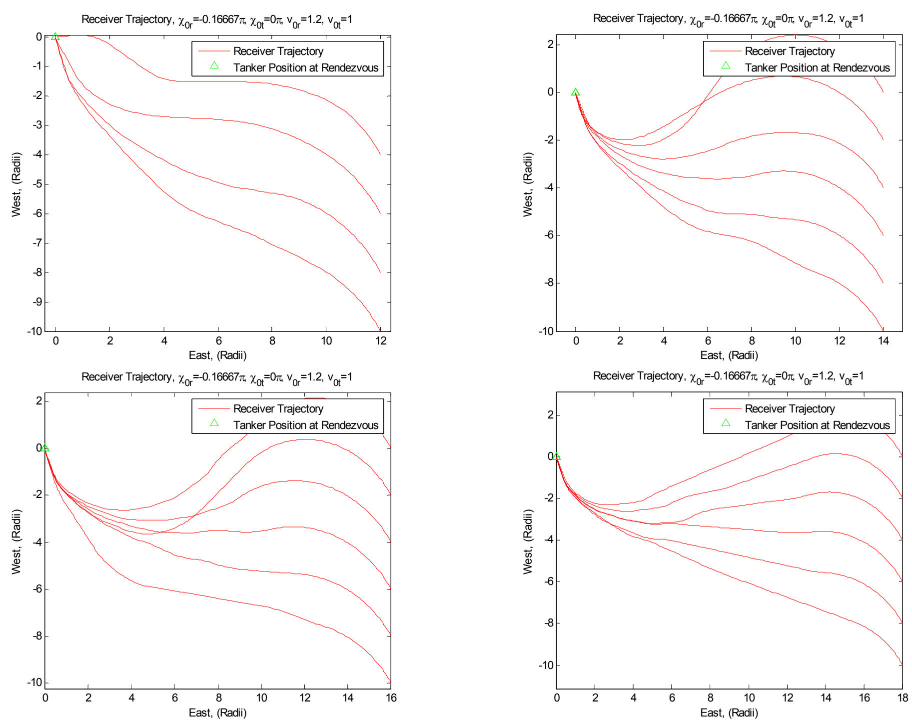

Figure 4-18 Trajectories with RTA=20

5. Conclusion

5.1. Overview

This section will present conclusions from this research as well as recommendation for further research.

5.2. Conclusions

The rendezvous controller developed using both Dubins geometric path planning and dynamic inversion shows promise as a method to effect an automated aerial refueling rendezvous. For large regions of the initial condition space, the controller is well behaved and compares very favorably with the dynamic optimization results. It effects a suitable rendezvous while following a trajectory that resembles a minimum distance, or Dubins, path and the path created by the dynamic optimization. Additionally, the velocity controller produces a bang-bang-like control that is optimal for the given scenario.

The region in which the controllers behave less satisfactorily or is unsuitable is well defined and understood. To fix the problem for these head-on scenarios, a controller could be designed that guides the receiver out of the corridor before handing over control to the rendezvous controller.

5.3. Recommendations

The following courses of action are recommended for further study.

1) For specified time rendezvous, the receiver should run the controller in the background while performing its mission so that the initial turn radius will be correctly sized when it begins executing the rendezvous. An ancillary benefit

is that the UAV will have a better estimate of the time/distance to the tanker and therefore will be able to decide when to stop its mission to refuel.

2) A low pass filter should be added to the velocity control loop of the minimum time model to increase the realism of the model.

3) In cases where the turn radius cannot be made large enough to expend the required amount of time, for example, when the receiver starts relatively close to the rendezvous point or when the receiver is already lined up for rendezvous, an auxiliary method for "wasting time" is needed. This method might simply consist of commanding an arbitrary turn until the rendezvous controller is able to effect the rendezvous at the required time.

4) Much could be done to improve the computational speed of the algorithm; for example using an optimization (minimization) routine to find the time at which the difference between the time to travel the tanker's path and the time to travel the receiver's path is zero. Additionally, some candidate paths may be eliminated by using methods proposed in *Shortest Path Synthesis for Dubins Non-holonomic Robot* [Bui 1994]. Reducing the number of candidate paths may significantly reduce the required computational power.

5) To increase the robustness of the model when used with a maneuvering tanker, recommend using tanker estimator to estimate the future position of the tanker, rather than projecting the current state. [Smith 2006]

6) Several measures should be taken to increase the realism of the simulation. A wind model should be added to the simulation to evaluate the controller in

changing winds. Also, noise should be added to the tanker state to simulate the receiver's imperfect knowledge. Finally, the controller should be tested using a six degree of freedom model.

Appendix A: Explanation of Code

Matrixizer.m

This function sets the initial conditions for various conditions spanning the solution space.

Initiator.m

This function passes the initial conditions to these functions, Dubins.m, dyn_opt.m, and controller.m.

Dubins.m

This function calculates the Dubins path from the receiver's initial position, to the calculated intercept point. This path is generated by recursively calling target_path.m and Dubins_path_maker.m to find the future position of the tanker at a future time and the time it takes to fly a Dubins path from the receiver's initial position to the future position of the tanker. When these times are the same, the calculated intercept point has been found.

Target_path.m

This function propagates the tanker position forward in time and returns the future position to Dubins.m.

Dubins_path_maker.m

This function generates a Dubins path from the receiver's initial position to a future tanker position and the associated travel time to that future position. The Dubins path is calculated by generating two circles of minimum turn radius tangent to the initial velocity

vector of the receiver and two circles of minimum turn radius tangent to the velocity vector of the projected. Lines tangent to each combination of initial and terminal circles are then constructed, resulting in four candidate paths. As long as the assumption holds, the shortest of these paths is the Dubins path. This assumption is that none of the circles overlap. Overlapping circles would result in the possibility that the Dubins path consists of three minimum radius turns rather than two minimum radius turns and a straight segment.

Dyn_opt.m

This function formulates the problem as a dynamic optimization problem and utilizes fmincon.m to solve the problem.

Controller.m

This function calls the Simulink model and passes in initial conditions. Additionally it receives the results from the model and passes them out to be plotted.

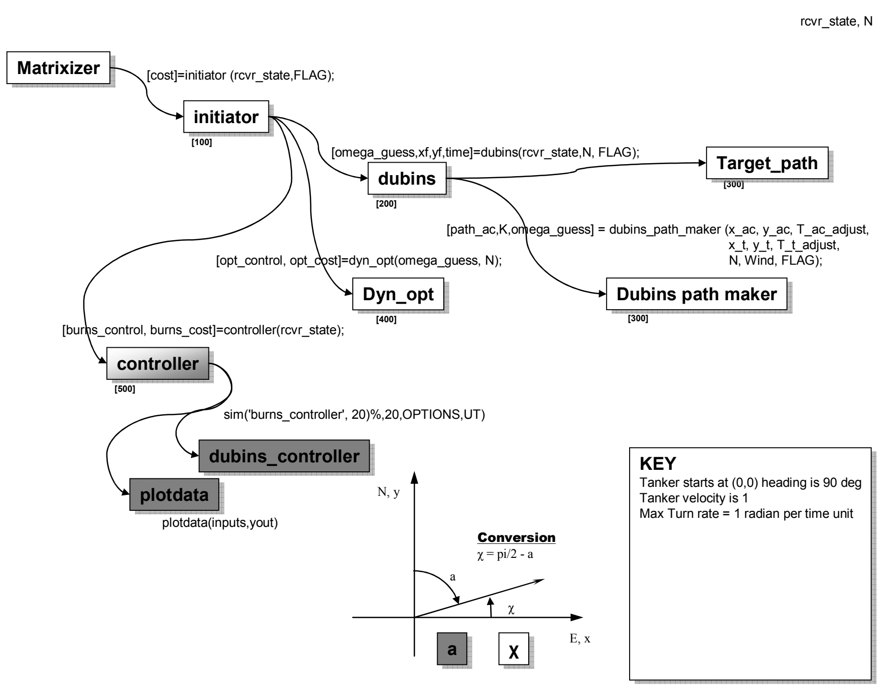

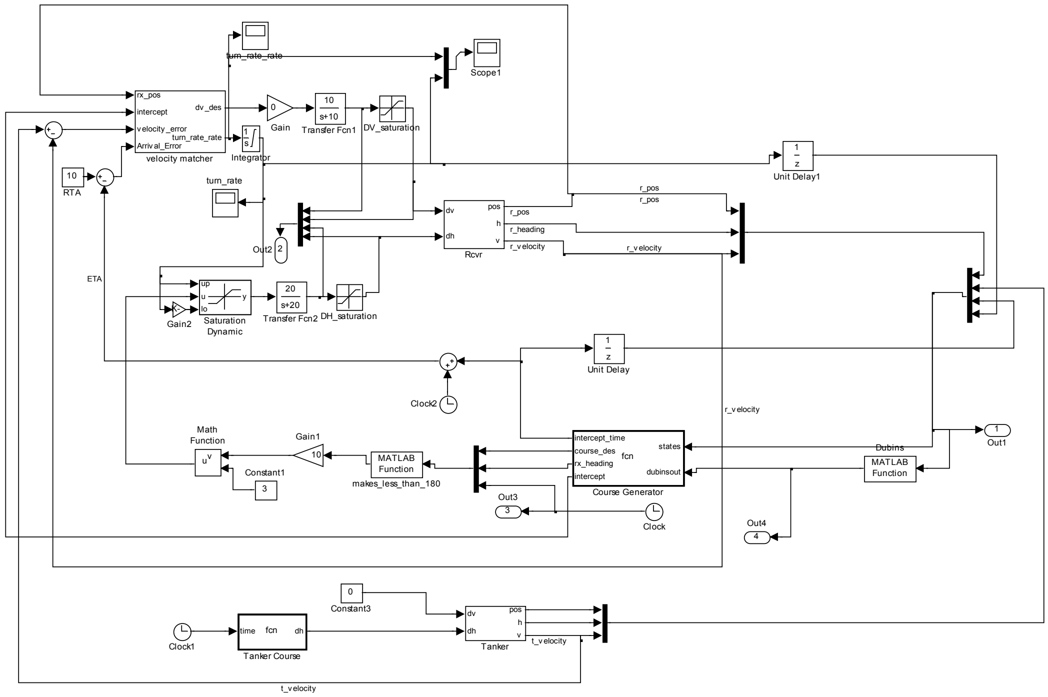

Minimum Time Controller

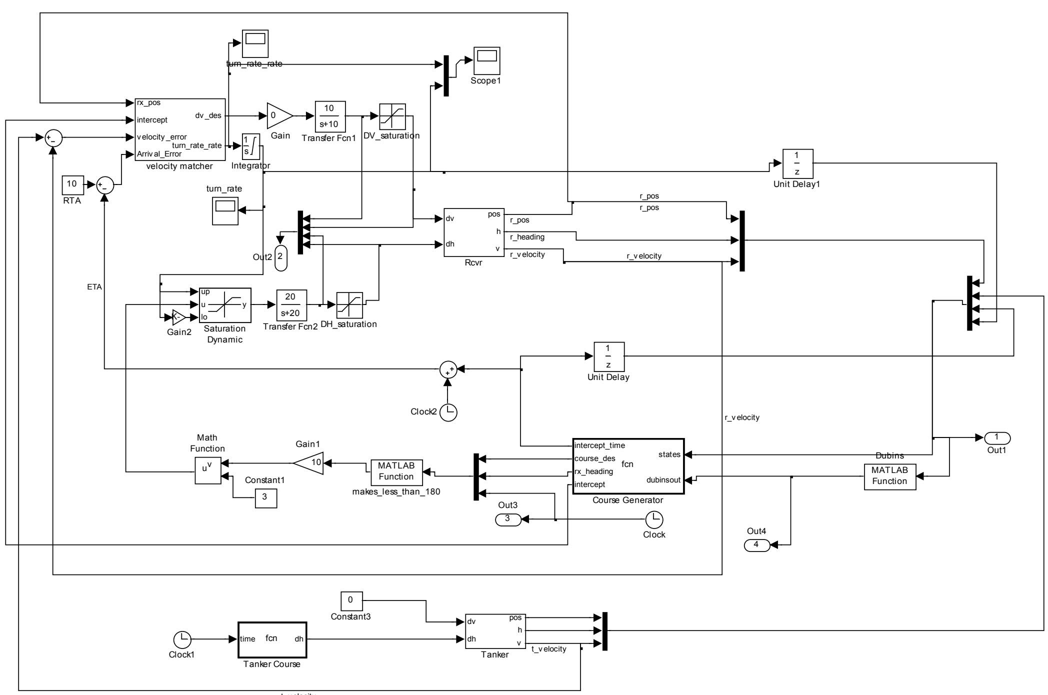

Specified Time Controller

Bibliography

1. Bui, X., Boissonnat, J., Soueres, P., Laumond, J., *Shortest Path Synthesis for Dubins Non-holonomic Robot*. IEEE, 1994

2. McGee, T., Spry, S., Hedrick, K., *Optimal path planning in a constant wind with bounded turning rate*, University of California, Berkeley. AIAA 2007

3. Ochi, Yoshimasa. Kominami, Takeshi, *Flight Control for Automatic Aerial Refueling via PNG and LOS Angle Control,* National Defense Academy, Kanagama. AIAA 2005

4. Smith, Austin, "PNG with Adaptive Terminal Guidance for Aircraft Rendezvous", Air Force Institute of Technology Presentation, 2006.

5. Steven M. Ross, Meir Pachter, and David R. Jacques, *Autonomous aerial refueling based on the tanker reference frame,* Air Force Institute of Technology, IEEE, 2006

6. Department of the Air Force. *Air Force Basic Doctrine.* AFDD-1. Washington: HQ USAF, 17 Nov 2003

7. Department of Defense. *Joint Doctrine and Joint Tactics, Techniques, and Procedures for Air Mobility Operations.* Joint Publication 3-17. Washington: 14 April 2006

8. Neilsen, M, *Air Refueling,* Elmendorf Air Force Base, *2005.*

9. Bryson, A. and Ho, Y., *Applied Optimal Control (Revised Printing)*. Hemisphere Publishing Co. 1975.

10. Gordon, Randel J. *"Optimal Dynamic Soaring for Full Size Sailplanes,"* AFIT Thesis AFIT/GAE/ENY06-S04 GAE 06S, (Sep 06)

11. Dubins, L. *On Curves of Minimal Length with a Constant on Average Curvature*, and with Prescribed Initial and Terminal Positions and Tangents. Carnegie Institute of Technology, 1957

12. Wright Laboratory. *Application of Multivariable Control Theory to Aircraft Control Laws*. Report WL-TR-96-3099, Wright-Patterson AFB May 1996

13. MATLAB Help File Version 7.1.0, The Mathworks Incorporated, 2 Aug 2005

14. Hull, D. *Conversion of Optimal Control Problems into Parameter Optimization Problems*. Journal of Guidance, Control, and Dynamics, Vol 20, No. 1, 1997

15. Jacques, Dave., *Functional Optimization and Optimal Control.* Air Force Institute of Technology, 2002

16. Larson, R., Mears, M., Blue, P., *Path Planning for Unmanned Air Vehicles to Goal States in Operational Environments*. AIAA, 2005

17. Larson, R., Pachter, M., Mears, M., *Path Planning by Unmanned Air Vehicles for Engaging an Integrated Radar Network*. AIAA Guidance, Navigation, and Control Conference and Exhibit. 2005-6191

18. Vaughn, A. *Path Planning and Control of Unmanned Aerial Vehicles in the Presence of Wind*. MS Thesis. Department of Mechanical Engineering, University of California at Berkeley, CA. Fall 2003.

Vita

Major Brian S. Burns graduated from the University of Kansas with a Bachelor of Science degree in Aeronautical Engineering in May 1995. He was commissioned through the Detachment 280 AFROTC at the University of Kansas. Upon commissioning, he was assigned as a test engineer to the Cruise Missile Product Group, Tinker AFB OK. While assigned to the Cruise Missile Product Group, he graduated from Oklahoma City University with a Master of Business Administration degree. In April 1998, he was assigned to the 10th Flight Test Squadron, where he performed the duty of a flight test engineer. In November 1999, he was assigned to the Air Force Operational Test and Evaluation Center, Kirtland AFB NM, where he served as lead analyst for bomber and air mobility systems. In November 2002, he was assigned to Detachment 2 645th Materiel Squadron, Greenville TX. In August 2005, he entered the Graduate School of Engineering and Management, Air Force Institute of Technology. Upon graduation, he will be assigned to Air Force Research Laboratory, Air Vehicles Directorate at Wright Field OH.

REPORT DOCUMENTATION PAGE

Form Approved
OMB No. 074-0188

1. REPORT DATE *(DD-MM-YYYY)*	**2. REPORT TYPE**	**3. DATES COVERED** *(From – To)*
22-03-2007	Master's Thesis	March 2006 – March 2007

4. TITLE AND SUBTITLE

AUTONOMOUS UNMANNED AERIAL VEHICLE RENDEZVOUS FOR AUTOMATED AERIAL REFUELING (AAR)

5a. CONTRACT NUMBER

5b. GRANT NUMBER

5c. PROGRAM ELEMENT NUMBER

6. AUTHOR(S)

Burns, Brian S., Maj, USAF

5d. PROJECT NUMBER

5e. TASK NUMBER

5f. WORK UNIT NUMBER

7. PERFORMING ORGANIZATION NAMES(S) AND ADDRESS(S)

Air Force Institute of Technology
Graduate School of Engineering and Management (AFIT/EN)
2950 Hobson Way, Building 640
WPAFB OH 45433-8865

8. PERFORMING ORGANIZATION REPORT NUMBER

AFIT/GAE/ENY/07-M05

9. SPONSORING/MONITORING AGENCY NAME(S) AND ADDRESS(ES)

AFRL/VAC
Dr. Jeffery Tromp
2130 Eighth St, WPAFB, OH 45433
937.255.3900

10. SPONSOR/MONITOR'S ACRONYM(S)

11. SPONSOR/MONITOR'S REPORT NUMBER(S)

12. DISTRIBUTION/AVAILABILITY STATEMENT

APPROVED FOR PUBLIC RELEASE; DISTRIBUTION UNLIMITED.

13. SUPPLEMENTARY NOTES

14. ABSTRACT

As unmanned aerial vehicles (UAVs) increase in capability, the ability to refuel them in the air is becoming more critical. Aerial refueling will extend the range, shorten the response times, and extend loiter time of UAVs. Executing aerial refueling autonomously will reduce the command and control, logistics, and training efforts associated with fielding UAV systems. Currently, the Air Force Research Lab is researching the various technologies required to conduct automated aerial refueling (AAR). One of the required technologies is the ability to autonomously rendezvous with the tanker. The goal of this research is to determine the control required to fly an optimum rendezvous using numerical optimization and to design a controller that will approximate that control. Two problems were examined. The first problem is for the receiver to rendezvous in minimum time, with a known tanker path. The second problem is for the receiver to rendezvous at a specified time with a known tanker path. For the first problem, the simulated controller results will be compared to the calculated optimal control.

15. SUBJECT TERMS

automated aerial refueling, uav, optimization, autonomous control, autonomous navigation, path planning, rendezvous,

16. SECURITY CLASSIFICATION OF:			**17. LIMITATION OF ABSTRACT**	**18. NUMBER OF PAGES**	**19a. NAME OF RESPONSIBLE PERSON**
a. REPORT	**b. ABSTRACT**	**c. THIS PAGE**			Paul Blue
U	U	U	UU	94	**19b. TELEPHONE NUMBER** *(Include area code)* (937) 255-6565, ext 7521 (paul.blue@afit.edu)

Standard Form 298 (Rev. 8-98)
Prescribed by ANSI Std. Z39-18